Disrupting D1-NMDA or D2-NMDA receptor heteromerization prevents cocaine's rewarding effects but preserves natural reward processing

Andry Andrianarivelo, Estefani Saint-Jour, Paula Pousinha, Sebastian P Fernandez, Anna Petitbon, Veronique de Smedt-Peyrusse, Nicolas Heck, Vanesa Ortiz, Marie-Charlotte Allichon, Vincent Kappès, et al.

NEUROSCIENCE

Disrupting D1-NMDA or D2-NMDA receptor heteromerization prevents cocaine's rewarding effects but preserves natural reward processing

Andry Andrianarivelo[1,2,3], Estefani Saint-Jour[1,2,3], Paula Pousinha[4,5], Sebastian P. Fernandez[4,5], Anna Petitbon[6], Veronique De Smedt-Peyrusse[6], Nicolas Heck[1,2,3], Vanesa Ortiz[4,5], Marie-Charlotte Allichon[1,2,3], Vincent Kappès[1,2,3], Sandrine Betuing[1,2,3], Roman Walle[6], Ying Zhu[7,8], Charlène Joséphine[9], Alexis-Pierre Bemelmans[9], Gustavo Turecki[10], Naguib Mechawar[10], Jonathan A. Javitch[7,8,11], Jocelyne Caboche[1,2,3], Pierre Trifilieff[6], Jacques Barik[4,5], Peter Vanhoutte[1,2,3]*

Addictive drugs increase dopamine in the nucleus accumbens (NAc), where it persistently shapes excitatory glutamate transmission and hijacks natural reward processing. Here, we provide evidence, from mice to humans, that an underlying mechanism relies on drug-evoked heteromerization of glutamate *N*-methyl-D-aspartate receptors (NMDAR) with dopamine receptor 1 (D1R) or 2 (D2R). Using temporally controlled inhibition of D1R-NMDAR heteromerization, we unraveled their selective implication in early phases of cocaine-mediated synaptic, morphological, and behavioral responses. In contrast, preventing D2R-NMDAR heteromerization blocked the persistence of these adaptations. Interfering with these heteromers spared natural reward processing. Notably, we established that D2R-NMDAR complexes exist in human samples and showed that, despite a decreased D2R protein expression in the NAc, individuals with psychostimulant use disorder display a higher proportion of D2R forming heteromers with NMDAR. These findings contribute to a better understanding of molecular mechanisms underlying addiction and uncover D2R-NMDAR heteromers as targets with potential therapeutic value.

INTRODUCTION

Drug addiction is characterized by compulsive patterns of drug-seeking and drug-taking behavior despite detrimental consequences and a high rate of relapse after abstinence. A hallmark of addictive drugs is their ability to increase dopamine (DA) concentration in discrete brain regions, which persistently shapes excitatory glutamate transmission within the reward circuit, thereby hijacking natural reward processing (*1*, *2*). This calls for a better understanding of the precise molecular events underlying the detrimental interplay between DA and glutamate signaling triggered by drugs of abuse.

The enduring behavioral alterations induced by protracted drug exposure are largely believed to result from persistent drug-evoked neuronal adaptations within the striatum, especially in its ventral part, the nucleus accumbens (NAc) (*1*, *3*). The striatum is indeed a key target structure of drugs of abuse that integrates convergent glutamate inputs from limbic, thalamic, and cortical regions, encoding components of drug-associated stimuli and environment, and DA signals that mediate reward prediction error and incentive values (*4*). Integration of DA and glutamate signals is achieved by the two segregated subpopulations of γ-aminobutyric acid–releasing (GABAergic) medium-sized spiny neurons (MSNs) expressing either the dopamine receptor (DAR) type 1 (D1R) or type 2 (D2R), although a fraction of MSN in the NAc expresses both receptors (*5*). Cell type–specific manipulations of neuronal activity showed that inhibiting and activating D1R-MSN dampen and potentiate long-term drug-evoked responses, respectively, in line with their "proreward" action (*2*, *6*–*9*). By contrast, most studies support an inhibitory role of D2R-MSN activation on drug-mediated adaptations (*6*, *7*, *10*–*12*). These studies, based on direct manipulations of MSN activity, were instrumental in highlighting the role of MSNs as putative players in drug-related behavioral adaptations. However, they do not establish how drugs of abuse persistently affect the functionality of each MSN subpopulation or the underlying cellular and molecular mechanisms. In this context, increasing evidence suggests that such a central role of MSN subpopulations in drug-induced behavioral adaptations originates, at least in part, from DA-dependent long-lasting changes at excitatory striatal synapses. Long-term potentiation of specific glutamatergic afferents impinging onto D1R-MSNs induced by DA is responsible for both the induction and maintenance of long-lasting behavioral adaptations to repeated cocaine exposure (*13*–*15*). Glutamate transmission onto D2R-MSNs seems to be spared by cocaine exposure but selectively altered during cocaine craving after long access to high doses of cocaine (*16*).

It is therefore timely to identify molecular mechanisms by which drug-evoked increases in DA can permanently hijack glutamate transmission onto MSNs. Although a number of studies have described the cross-talk between D1R and glutamate receptors of the

[1]CNRS, UMR 8246, Neuroscience Paris Seine, F-75005 Paris, France. [2]INSERM, UMR-S 1130, Neuroscience Paris Seine, Institute of Biology Paris Seine, F-75005 Paris, France. [3]Sorbonne Université, UPMC Université Paris 06, UM CR18, Neuroscience Paris Seine, F-75005 Paris, France. [4]Université Côte d'Azur, Nice, France, [5]Institut de Pharmacologie Moléculaire et Cellulaire, CNRS UMR7275, Valbonne, France. [6]Université Bordeaux, INRAE, Bordeaux INP, NutriNeuro, 33000 Bordeaux, France. [7]Division of Molecular Therapeutics, New York State Psychiatric Institute, New York, NY 10032, USA. [8]Department of Psychiatry, Columbia University, New York, NY 10032, USA. [9]Commissariat à l'Énergie Atomique et aux Énergies Alternatives (CEA), Département de la Recherche Fondamentale, Institut de biologie François Jacob, MIRCen, and CNRS UMR 9199, Université Paris-Sud, Université Paris-Saclay, Neurodegenerative Diseases Laboratory, Fontenay-aux-Roses, France. [10]Douglas Mental Health University Institute, Department of Psychiatry, McGill University, Montreal, QC, Canada. [11]Department of Pharmacology, Columbia University, New York, NY 10032, USA.
*Corresponding author. Email: peter.vanhoutte@sorbonne-universite.fr

N-methyl-D-aspartate (NMDAR) subtype as a key player in the behavioral effects of psychostimulants (*2*, *17*–*22*), the underlying molecular mechanisms remain elusive. Moreover, the processes by which DA impairs D2R-MSN activity to promote long-lasting drug-induced reinforcement are yet unknown.

Heteromeric complexes formed between DARs and glutamate NMDAR have been proposed as integrators of DA and glutamate signals in both MSN populations (*23*). Receptor heteromers are of particular interest not only because of their ability to dynamically modulate the component receptor's functions in time and space but also because they exhibit functional properties distinct from the component receptors, making them attractive targets for the development of more selective pharmacological strategies (*24*–*27*). Most evidence generated to date regarding DAR-NMDAR heteromers' functions comes from in vitro and ex vivo studies, and their potential role in long-term drug-induced adaptations has been overlooked. D1R heteromers formed with glutamate ionotropic receptor NMDA type subunit 1 (GluN1) subunits of NMDAR have been described in vitro (*28*, *29*) and ex vivo in the striatum (*30*, *31*). We established that acutely perturbing D1R-NMDAR interaction blunts the facilitation of NMDAR signaling by DA in D1R-MSN in striatal slices, as well as cocaine-induced locomotor sensitization (*31*). However, the impact of chronic disruption of D1R-NMDAR on the sensitizing and rewarding effects of repeated cocaine exposure is unknown. In contrast, the interaction of D2R with GluN2B subunits of NMDAR has been shown to mediate the inhibition of NMDA currents by DA in D2R-MSNs and control acute stereotypic locomotor responses to high cocaine doses (*32*). Nonetheless, the implication of D2R-NMDAR heteromerization in long-lasting behavioral alterations induced by cocaine has not been studied. However, D2R-dependent transmission is largely believed to be a main actor in the development of addiction based on clinical and preclinical findings (*2*, *33*).

We therefore investigated whether heteromers formed by DAR and NMDAR constitute molecular substrates by which drugs of abuse enduringly alter glutamate transmission and mediate long-lasting sensitizing and rewarding effects of cocaine. We found that repeated cocaine exposure triggers a transient increase in D1R-NMDAR heteromerization throughout the entire striatum, which returns to baseline after an abstinence period. By contrast, cocaine induces a stable increase in heteromerization of D2R-NMDAR that is mostly restricted to the NAc and persists over 7 days of abstinence. Using a temporally controlled disruption of these receptor heteromers, combined with electrophysiological recordings, imaging, and behavioral assessments, we showed that D1R-NMDAR heteromerization controls the development of cocaine-evoked long-term synaptic plasticity and morphological changes in D1R-MSNs, as well as behavioral adaptations. D2R-NMDAR heteromerization not only contributes to the development of the sensitizing and rewarding effects of cocaine but, more importantly, also mediates the persistence of these adaptations after a period of abstinence, followed by a reexposure to the drug. The targeting of either type of heteromers preserves natural reward processing. Notably, we found that these receptor complexes also exist in human postmortem brain samples and showed that, despite a substantial decrease in D2R protein expression, individuals with a history of psychostimulant use disorder display a significantly higher proportion of D2R that form heteromers with GluN2B-containing NMDAR in the NAc. Our results support a model by which the heteromerization of DA and glutamate receptors induced by drugs of abuse in D1R- and D2R-MSNs is a key molecular event underlying the detrimental interplay between these two neurotransmitter systems in drug addiction. The role of D2R-NMDAR heteromers in the persistence of the sensitizing and rewarding effects of drugs makes them potential targets not only for treating addiction in humans but also, more broadly, in multiple neuropsychiatric disorders.

RESULTS

Detection and temporally controlled disruption of striatal D1R-NMDAR and D2R-NMDAR heteromerization in vivo

A prerequisite for the study of DAR-NMDAR heteromer modulation and function in cocaine-evoked adaptations was to develop approaches to both visualizing and interfering with receptor interactions in vivo. Detection of endogenous D1R-NMDAR proximity was first assessed in the NAc of naïve mice through proximity ligation assay (PLA) (*34*). The bright-field PLA assay yielded a brown punctate signal for D1R-NMDAR complexes that was absent when one of the two primary antibodies was omitted (Fig. 1A), similar to what was previously found when PLA was performed in D1R receptor knockout mice (*31*). To study the function of D1R-NMDAR heteromers, we designed an adeno-associated virus (AAV)–based strategy to disrupt heteromers in a spatially and temporally controlled manner (Fig. 1B). The AAV-Tet-On-GluN1C1 allows a doxycycline (dox)–inducible bicistronic expression of the red fluorescent protein (RFP) reporter protein together with a peptide corresponding to the C1 cassette (D_{864}-T_{900}) of GluN1 that binds to D1R (*28*). This peptide blocks D1R-NMDAR interaction in vitro while preserving the functions of individual D1R and NMDAR independently of their heteromerization (*31*). The control virus, Tet-On-GluN1C1Δ, encodes a C1 cassette deleted of nine amino acids that are required for electrostatic interactions between D1R and GluN1 (*35*). This mutated cassette does not interfere with D1R-GluN1 interaction in vitro (*31*). After stereotaxic injections in the NAc, the treatment with dox triggered a rapid and sustained expression of the RFP reporter (Fig. 1B). Analysis of D1R-NMDAR proximity in RFP-positive neurons showed that Tet-On-GluN1C1 significantly reduced D1R-NMDAR PLA puncta when compared to the control AAV (Fig. 1, C and D). Notably, we also verified that blocking D1R-NMDA heteromerization altered downstream cocaine-mediated signaling events (*20*, *31*), including GluN2B phosphorylation and extracellular signal–regulated kinase pathway activation (fig. S1), without compromising neuronal survival (Fig. 1E). As for D1R-NMDAR heteromers, bright-field PLA detection of D2R-NMDAR proximity appeared as a brown punctate signal, which disappeared upon omission of one primary antibody (Fig. 1F). To interfere with D2R-NMDAR interaction, we generated AAV-Tet-On-D2R-IL3, which drives a dox-inducible expression of a peptide corresponding to a small fragment (T_{225}-A_{234}) located within the third intracellular loop (IL3). This IL3 domain is known to play a key role for D2R-NMDAR interaction (*32*). Since critical amino acids responsible for D2R-NMDAR interaction have not been yet identified within this D2R-IL3 fragment, we used a control virus (Tet-On-D2R-IL3-scr) driving the expression of a scrambled peptide (Fig. 1G). We found that Tet-On-D2R-IL3 efficiently reduced D2R-NMDAR PLA puncta (Fig. 1, H and I) while preserving neuronal survival (Fig. 1J). Together, these results validate both an efficient disruption of receptor heteromerization and the accuracy of using PLA to detect DAR-NMDAR heteromers in vivo.

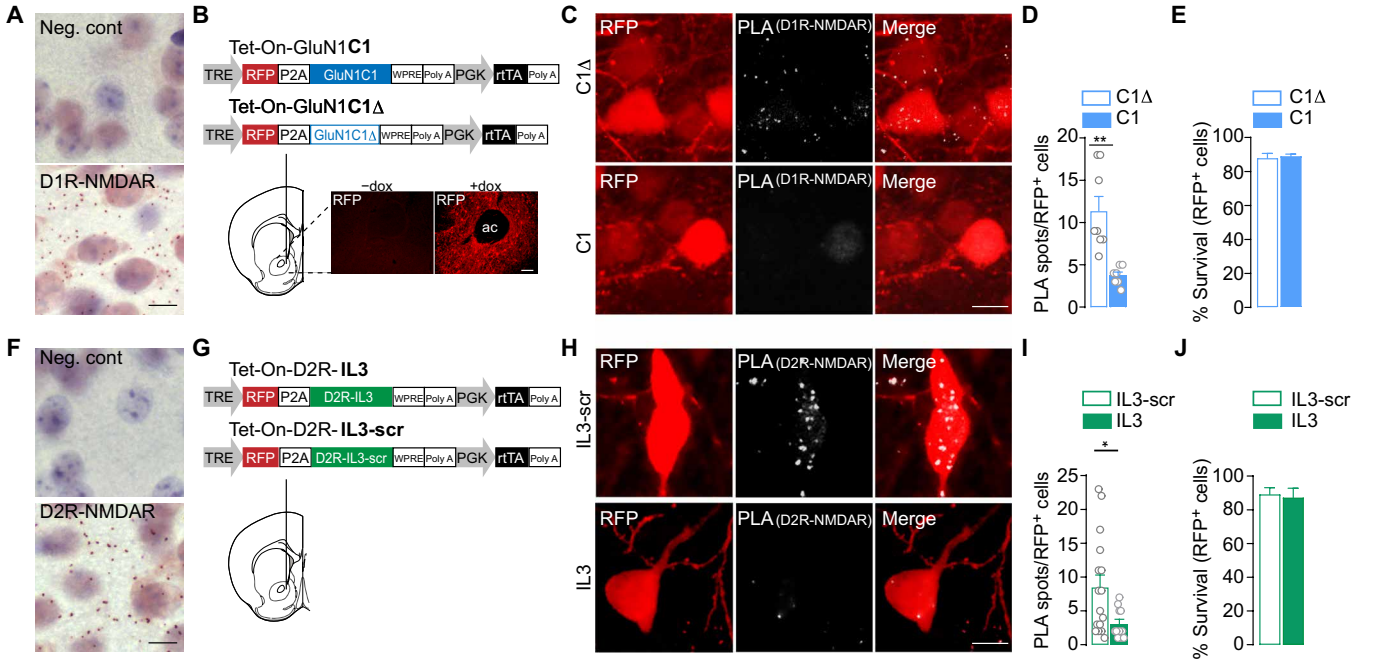

Fig. 1. Detection and temporally controlled disruption of striatal D1R-NMDAR and D2R-NMDAR heteromerization in vivo. (**A**) Example images of D1R-NMDAR heteromer PLA detection and related negative (Neg. cont) showing the absence of signal when one primary antibody is omitted. (**B**) Top: Viral-based strategy for expression of interfering peptide to disrupt D1R-NMDAR interaction [Tet-On-GluN1C1 (C1)] and control [Tet-On-GluN1C1Δ (C1Δ)] in the NAc. Bottom: Example image of dox (+dox)–mediated RFP expression [anterior commissure (ac)]. TRE, tetracycline response element; P2A, 2A peptide; PGK, phosphoglycerate kinase 1 promoter; rtTA, reverse tetracycline-controlled transactivator. (**C**) Example image of D1R-NMDAR heteromer detection by PLA in C1Δ- and C1-transduced neurons. (**D**) Quantifications of the fluorescent PLA signal in C1Δ- and C1-transduced neurons. Two-sided Student's *t* test, $t = 4.078$, df = 13, $^{**}P = 0.0013$, $n = 7$ to 8 cells from four mice per group. (**E**) Neuronal survival of C1Δ- and C1-transduced neurons. Two-sided Student's *t* test, $t = 0.354$ df = 6, $P = 0.735$, $n = 4$ mice per group. (**F**) Same as in (A), for D2R-NMDAR heteromer PLA detection. (**G**) Viral strategy for expression of interfering peptide to prevent D2R-NMDAR heteromerization [Tet-On-D2R-IL3 (IL3)] and control [Tet-On-D2R-IL3-scr (IL3-scr)]. (**H**) Representative image D2R-NMDAR heteromer detection by PLA in IL3-scr– and IL3-transduced neurons. (**I**) Quantifications of the fluorescent PLA signal in IL3-scr– and IL-3 infected neurons. Two-sided Student's *t* test, $t = 2.393$, df = 25, $^{*}P = 0.0246$, $n = 11$ to 16 cells from 4 mice per group. (**J**) Neuronal survival of IL3-scr– and IL3-transduced neurons. Two-sided Student's *t* test, $t = 0.2767$ df = 6, $P = 0.7913$, $n = 4$ mice per group. Scale bars, 10 μm. Error bars denote SEMs.

Behavioral sensitization to cocaine is associated with transient D1R-NMDAR heteromerization and prolonged D2R-NMDAR heteromerization in the NAc

We investigated whether a cocaine regimen that triggers persistent behavioral adaptations can modulate the formation of these receptor complexes in vivo in the striatum. Mice were subjected to five daily injections of cocaine (15 mg/kg), which elicits a progressive locomotor sensitization (Fig. 2A) that is known to persist despite several weeks of abstinence. This behavioral paradigm is a straightforward model to study the mechanisms involved in drug-induced behavioral adaptations (*2*, *36*). Mice were euthanized 1 day after the last injection to detect endogenous DAR-NMDAR proximity in distinct striatal subregions through PLA (*34*). We found that cocaine-treated mice displayed increased D1R-NMDAR heteromerization in the dorsolateral striatum (DL Str) and dorsomedial striatum (DM Str), as well as in the NAc core and NAc shell subdivisions (Fig. 2B). Cocaine also increased D2R-NMDAR heteromerization, but primarily in the NAc, with a smaller effect in the DL Str (Fig. 2C). This increased heteromerization occurred in the absence of changes in global expression levels of the component receptors (fig. S2A,B). Notably and as previously observed (*37*), repeated cocaine exposure decreases expression levels of the synaptic scaffold protein postsynaptic density 95 (PSD-95) (fig. S2C), which could partly explain our results as the interaction of NMDAR and D1R with PSD-95, through partly overlapping domains, has been described to prevent D1R-NMDAR interaction (*38*).

To study the kinetics of receptor heteromerization, mice were subjected to a cocaine-induced locomotor sensitization paradigm, followed by 1-week abstinence period and a challenge injection of saline or cocaine. We found that cocaine-mediated D1R-NMDAR heteromerization was transient, as it returned to baseline levels after 7 days of abstinence in the NAc core, DM Str, and DL Str and was significantly decreased below saline-treated mice in the NAc shell. After a challenge injection of cocaine, D1R-NMDAR heteromerization increased again in all striatal subregions except in the DL Str, after the challenge injection of cocaine (Fig. 2D). Notably, D2R-NMDAR heteromerization appeared to be sustained (15 ± 3.5% compared to the saline-treated group) over the abstinence period, specifically in the NAc core. The challenge injection of cocaine further increased D2R-NMDAR heteromers in the NAc, but not in dorsal parts of the striatum (Fig. 2D). To assess the role of D1R or D2R stimulation for receptor heteromerization, mice underwent a cocaine-locomotor sensitization followed by an abstinence period. Before a cocaine challenge, mice received an intraperitoneal injection of D1R or D2R antagonist that blunted the expression of behavioral sensitization. This allowed us to show that the stimulation

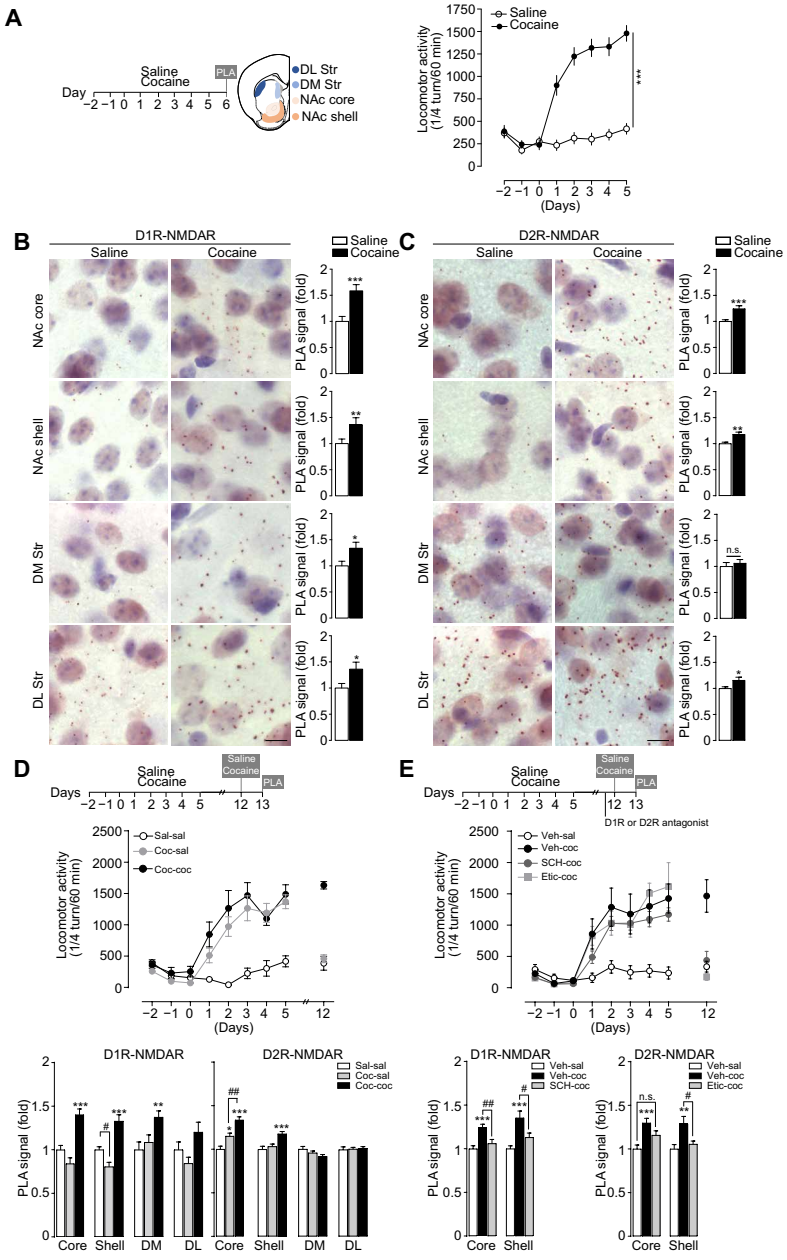

Fig. 2. Behavioral sensitization to cocaine is associated with transient D1R-NMDAR heteromerization and prolonged D2R-NMDAR heteromerization in the NAc. (**A**) Experimental time frame [NAc core and NAc shell and measurements of locomotor activity before and during 5 days of saline or cocaine (15 mg/kg) injections]. Two-way analysis of variance (ANOVA): treatment effect, $F_{1,24} = 67.79$, $^{***}P < 0.0001$ saline versus cocaine on day 5, $n = 13$ mice per group. DM, dorso-medial striatum; DL, dorso-lateral striatum. (**B**) Detection and quantifications of D1R-NMDAR heteromerization in saline- and cocaine-treated groups. PLA signal is represented as fold increase normalized to the saline group. Two-sided Student's *t* test: $^{*}P < 0.05$, $^{**}P < 0.01$, and $^{***}P < 0.001$ (saline versus cocaine); $n = 28$ to 84 fields of view per structure (NAc core, 4; NAc shell, 12; DM, 6; DL, 6; fields of view per mice) from seven mice per group. (**C**) Same as for (B) for D2R-NMDAR heteromerization. (**D**) Experimental time frame, measurements of locomotor activity, and quantifications of D1R-NMDAR and D2R-NMDAR heteromerization. PLA signal is represented as fold increase normalized to the saline group. One-way ANOVA: $^{*}P < 0.05$, $^{**}P < 0.01$, and $^{***}P < 0.001$ (saline-saline versus cocaine-saline/cocaine-cocaine); $\#P < 0.05$ and $\#\#P < 0.01$ (cocaine-saline versus cocaine-cocaine); $n = 28$ to 84 fields of view per structure from seven mice per group. (**E**) Same as for (D) except that mice received either a vehicle solution (Veh) or the D1R antagonist SCH23390 (SCH) or the D2R antagonist eticlopride (Etic) before a cocaine challenge. One-way ANOVA: $^{**}P < 0.01$ and $^{***}P < 0.001$ (vehicle-saline versus vehicle-cocaine); $\#P < 0.05$ and $\#\#P < 0.01$ (vehicle-cocaine versus SCH-cocaine or cocaine versus Etic-cocaine); n.s., not significant; $n = 28$ to 84 fields of view per structure from seven mice per group. Scale bars, 10 μm (B and C). Error bars denote SEMs.

of D1R or D2R was essential for cocaine-induced D1R-NMDAR and D2R-NMDAR heteromerization, respectively (Fig. 2E). Together, these data show that behavioral sensitization to cocaine is associated with a DAR-dependent transient heteromerization of D1R-NMDAR throughout the whole striatum, whereas D2R-NMDAR heteromerization occurs primarily in the NAc and is maintained in the core subdivision during a 7-day abstinence from cocaine.

Cocaine-evoked potentiation of glutamate transmission onto D1R-MSNs requires D1R-NMDAR heteromerization

Long-lasting changes of glutamate transmission at cortical projections onto D1R-MSN of the NAc have been causally implicated in the development of cocaine-induced locomotor sensitization (*13*). To study the contribution of D1R-NMDAR heteromerization to drug-induced plasticity at these synapses, we injected mice with Tet-On-GluN1C1 together with a mixture of AAV-PPTA-Cre, driving the expression of the Cre recombinase under the control of the D1R-MSN–specific preprotachykinin (PPTA) promoter, and AAV-Double-floxed inverse Open reading frame (DIO)–eGFP (enhanced green fluorescent protein) to tag D1R-MSN (fig. S3A) (*7*, *39*, *40*). These mice were supplemented with dox before and during daily injections of saline or cocaine for 5 days, followed by a 10-day abstinence period. As previously shown (*16*), cocaine triggered an increase in AMPA/NMDA (A/N) ratio, an index of synaptic plasticity, in D1R-MSN of mice injected with the control virus in the NAc. By contrast, while preserving basal synaptic transmission in the saline-treated group, the inhibition of D1R-GluN1 heteromerization blunted the cocaine-evoked increase in A/N ratio (Fig. 3, A and B), without modifying the amplitude or the kinetics of NMDAR excitatory postsynaptic currents (EPSCs; Fig. 3, C and D). These data show that D1R-NMDAR heteromerization controls cocaine-evoked changes in glutamate transmission in D1R-MSNs.

D1R-NMDAR heteromerization controls the development of cocaine-induced locomotor sensitization

We next evaluated the role of D1R-NMDAR heteromerization in the behavioral sensitizing properties of cocaine by supplementing Tet-On-AAV–injected mice with dox before and during saline or cocaine administration (Fig. 3E). Uncoupling D1R from GluN1 subunits of NMDAR did not affect basal locomotion nor the acute hyperlocomotor

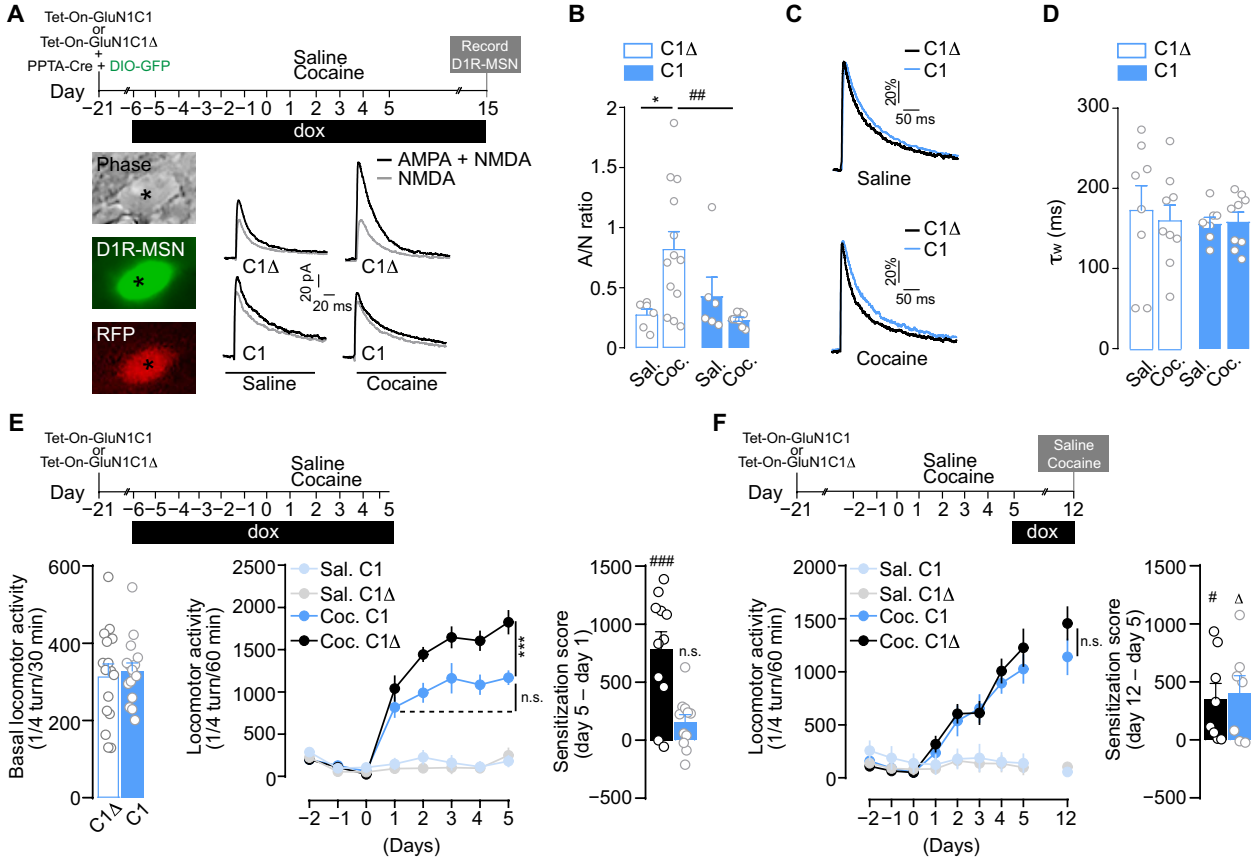

Fig. 3. D1R-NMDAR heteromerization controls cocaine-evoked potentiation of glutamate transmission onto D1R-MSN and the development of behavioral sensitization. (**A**) Experimental design and example trace of AMPA+NMDA (black) and NMDA (gray) currents in neurons (asterisk) expressing GFP [i.e., D1R-MSN (see fig. S3A)], and C1 or C1Δ (RFP$^+$). (**B**) A/N ratios. Two-way ANOVA: virus effect, $F_{1,30} = 2.511$, $^*P = 0.033$ and $\#\#P = 0.0061$, $n = 3$ to 4 mice per group and $n = 6$ to 13 cells per group. (**C**) Comparison of representative recordings of pharmacologically isolated NMDAR EPSCs, normalized to the peak amplitude (in percentage). (**D**) Deactivation kinetics of NMDAR EPSCs. Two-way ANOVA: virus effect, $F_{1,30} = 0.205$, $P > 0.999$, $n = 3$ to 4 mice per group and $n = 8$ to 9 cells per group. (**E**) Top: Experimental time frame and basal locomotor activity. Bottom left: Two-sided Student's t test, $t = 0.332$ df = 30, $P = 0.742$, $n = 16$ mice per group. Bottom middle: Inhibition of D1R-NMDAR heteromerization during the development of locomotor sensitization. Three-way ANOVA: virus effect, $F_{1,256} = 13.72$, $^{***}P = 0.0003$; n.s., $P > 0.9999$; n = 7 to 11 mice per group. Bottom right: Sensitization scores of cocaine-treated mice injected with Tet-On-GluN1C1Δ (black) or Tet-On-GluN1C1 (blue). One-sample Student's t test: $t = 5.289$, df = 10, $\#\#\#P = 0.0004$ (cocaine C1Δ versus 0); $t = 2.197$; df = 10; n.s., $P > 0.05$ (cocaine C1 versus 0). (**F**) Top: Experimental time frame. Bottom left: Inhibition of D1R-NMDAR heteromerization during 7 days of abstinence, followed by a challenge cocaine injection. Three-way ANOVA: virus effect, $F_{1,243} = 0.6160$, $P > 0.9999$, $n = 7$ to 8 mice per group. Bottom right: Sensitization scores of cocaine-treated mice injected with Tet-On-GluN1C1Δ (black) or Tet-On-GluN1C1 (blue). One-sample Student's t test, $t = 5.289$, df = 7, $\#P = 0.0325$ (cocaine C1Δ versus 0); $t = 2.599$, df = 6, $\Delta P = 0.0407$ (cocaine C1 versus 0). Error bars denote SEMs.

response triggered by the first cocaine injection but fully blocked the development of the behavioral sensitization induced by subsequent injections (Fig. 3E). Notably, dox supplementation did not alter body weight, basal locomotion, or behavioral sensitization to cocaine in mice that were not injected with Tet-On viruses (fig. S4, A to C).

By temporally controlling expression of the interfering peptides, we assessed the contribution of D1R-NMDAR heteromerization to the maintenance phase of locomotor sensitization. Mice injected with Tet-On viruses were treated with saline or cocaine for 5 days in the absence of dox. As expected, these mice displayed a similar cocaine-induced locomotor sensitization regardless of the virus injected. To switch off D1R-NMDAR heteromerization after behavioral sensitization, dox was given after the last saline or cocaine injection and during a 7-day abstinence period, followed by a challenge injection of saline or cocaine (Fig. 3F, top). We found that mice displayed the same level of sensitization in response to the cocaine challenge regardless of the AAV used, demonstrating that D1R-NMDAR heteromerization is not required for the maintenance of locomotor sensitization (Fig. 3F, bottom). Since cocaine also enhanced D1R-NMDAR heteromerization in the dorsal striatum (Fig. 2B), we also targeted heteromers in this striatal subregion and obtained the same results (fig. S4, D and E). Overall, these data show that D1R-NMDAR heteromerization in the striatum controls the development, but not the maintenance, of cocaine's sensitizing effects.

D2R-NMDAR heteromerization is involved in the development and maintenance of cocaine's sensitizing effects

In light of the significant and persistent impact of cocaine on D2R-NMDAR heteromerization in the NAc (Fig. 2, C to E), we studied the consequences of disrupting D2R-NMDAR interaction on glutamate transmission onto D2R-MSN and on the sensitizing effects of cocaine using AAV-Tet-On-D2R-IL3 (see Fig. 1, G to I). Because repeated cocaine exposure does not modify A/N ratio in D2R-MSN (*16*), the influence of uncoupling D2R from NMDAR was studied in saline-treated animals with virally tagged D2R-MSN owing to the coinjection of AAV-PPE-Cre, driving the expression of the Cre recombinase under the control of the D2R-MSN–specific preproenkephalin (PPE) promoter (*7*) and AAV-DIO-eGFP (fig. S3B). We found that inhibiting D2R-NMDAR heteromerization did not alter, by itself, A/N ratio in D2R-MSN (Fig. 4, A and B). The AAV-Tet-On-D2R-IL3 also left unchanged the amplitude and kinetics of NMDA currents (Fig. 4, C and D), indicating a lack of nonspecific effects of our strategy on NMDAR functionality. Notably, disrupting D2R-NMDAR interaction with AAV-Tet-On-D2R-IL3 also spared the ability of a D2R agonist to inhibit cyclic adenosine-3′,5′-monophosphate (cAMP) production in a heterologous system (Fig. 4E), demonstrating that our interfering strategy selectively perturbs D2R-NMDAR heteromerization while preserving the functions of individual component receptors.

At the behavioral level, interfering with D2R-NMDAR heteromerization preserved basal locomotion but blunted the development of cocaine-induced locomotor sensitization (Fig. 4F). Notably, as opposed to D1R-NMDAR complexes, we found that the inhibition of D2R-NMDAR heteromerization during the abstinence period also reduced the maintenance of the behavioral sensitization compared to cocaine-treated mice injected with the control virus (Fig. 4G). These mice were euthanized 24 hours after the last cocaine exposure to analyze expression levels of ΔFosB, which has been shown to be persistently expressed in response to cocaine (*41*). Although modulating ΔFosB expression levels in D2R-MSN has been shown to not affect behavioral responses to cocaine (*42*–*44*), ΔFosB expression was used here as a readout for potential signaling and transcriptional alterations induced in D2R-MSN as a consequence of D2R-NMDAR heteromer disruption during abstinence and reexposure to cocaine. Notably, we observed a significant increase in the number of ΔFosB-positive D2R-MSN after the cocaine challenge upon inhibition of D2R-NMDAR interaction (fig. S5A). This suggests that D2R-NMDAR heteromer disruption is associated with signaling pathway activation in D2R-MSN. Regardless, these data demonstrate that D2R-NMDAR heteromerization controls both the development and the maintenance of cocaine's sensitizing effects.

Differential roles of D1R-NMDAR and D2R-NMDAR heteromers in controlling the rewarding effects of cocaine

We next investigated the role of these heteromers in the rewarding effects of cocaine using a conditioned place preference (CPP) paradigm. Mice injected in the NAc with a control virus and supplemented with dox developed a significant cocaine-induced CPP, which was blunted when D1R and NMDAR were uncoupled (Fig. 5A). Although single or repeated cocaine administration has been shown to trigger dendritic spine formation in D1R-MSN (*39*, *45*), there is no study showing these morphological changes in the NAc in the context of CPP. Mice were thus euthanized the day after the behavioral test to perform a three-dimensional morphological analysis of GFP-tagged D1R-MSN. Control mice, which developed CPP to cocaine, displayed a significant increase in dendritic spine density in D1R-MSN, which was inhibited when D1R and NMDAR were uncoupled (Fig. 5B). To study the implication of D1R-NMDAR heteromerization on cocaine-induced reinstatement of CPP, AAV-injected mice were initially trained for CPP in the absence of dox. Once mice developed CPP, dox was added to alter D1R-NMDAR interaction during an extinction period, followed by a cocaine-induced reinstatement of CPP. We observed that the inhibition of D1R-NMDAR interaction did not alter the kinetics of extinction nor the reinstatement of CPP (Fig. 5C), thus supporting a critical role for D1R-NMDAR heteromers in the development of the rewarding effects of cocaine, as observed for locomotor sensitization, but not in the extinction or reinstatement of CPP.

The uncoupling of D2R from NMDAR also blocked the development of cocaine CPP (Fig. 5D), but this was not correlated to morphological changes in D2R-MSNs since the CPP paradigm did not trigger any modification of dendritic spine density in D2R-MSN regardless of the AAV used (Fig. 5E). Inhibiting D2R-NMDAR heteromerization once the mice had developed CPP did not affect the extinction of CPP but significantly reduced cocaine-induced reinstatement of CPP (Fig. 5F). Notably, this inhibitory effect of D2R-NMDAR heteromer disruption on cocaine-induced reinstatement of CPP was associated with an increased expression of ΔFosB in D2R-MSN (fig. S5B), similar to what we observed after a challenge injection of cocaine in the locomotor sensitization paradigm.

Together, these results indicate that D2R-NMDAR heteromerization is required for both the development and reinstatement of cocaine-induced CPP, independently of morphological changes in GFP-tagged D2R-MSNs.

Inhibiting D1R-NMDAR or D2R-NMDAR heteromerization does not alter CPP for food

Manipulating D1R-NMDAR or D2R-NMDAR heteromerization in vivo allowed us to reveal their selective implication in controlling

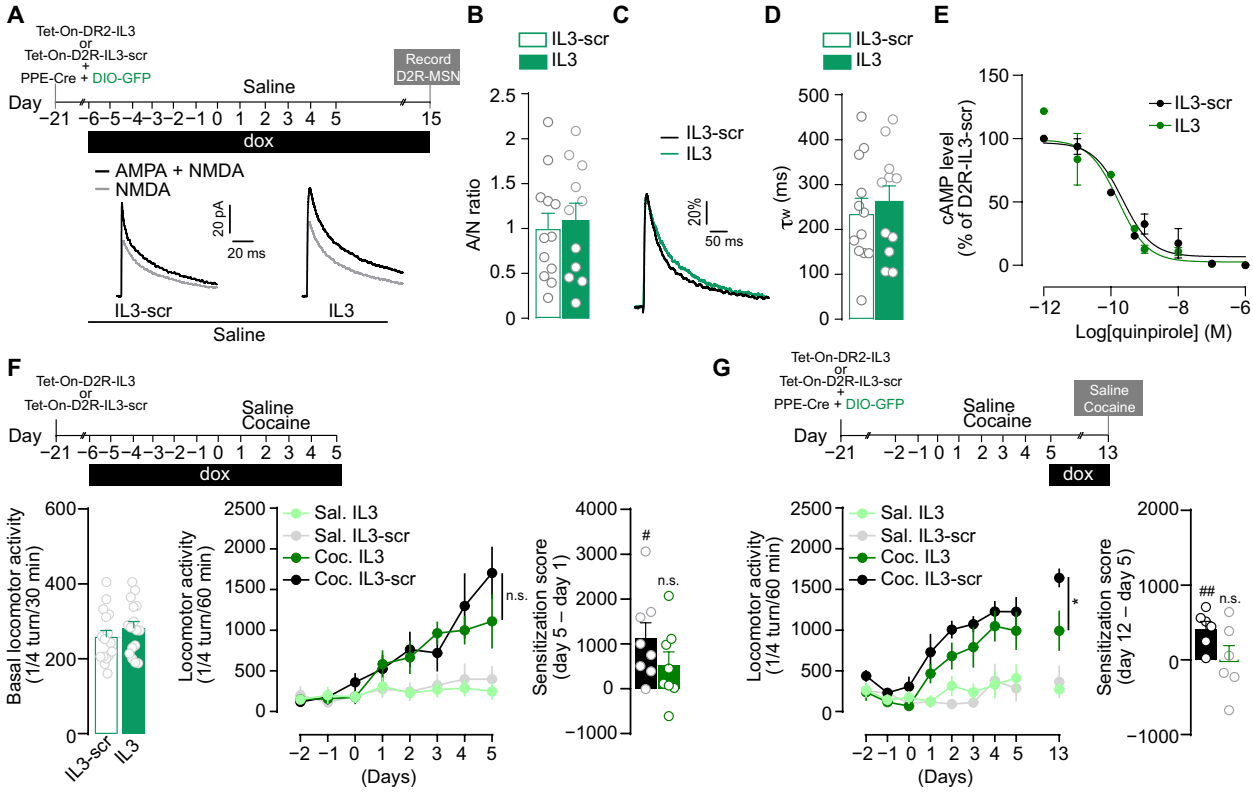

Fig. 4. D2R-NMDAR heteromerization is involved in the development and maintenance of cocaine's sensitizing effects. (**A**) Experimental time frame and representative traces of AMPA + NMDA (black) and NMDA (gray) currents in neurons expressing GFP [i.e., D2R-MSN (see fig. S3B)] and IL3 or IL3-scr (RFP$^+$) (**B**) A/N ratios. Two-sided Student's *t* test: $t = 0.3397$, df = 21, $P = 0.7375$, $n = 4$ to 6 mice per group and $n = 11$ to 12 cells per group. (**C**) Comparison of representative recordings of pharmacologically isolated NMDAR EPSCs, normalized to the peak amplitude (in percentage). (**D**) Deactivation kinetics of NMDA EPSCs. Two-sided Student's *t* test: $t = 0.5129$, df = 21, $P = 0.6134$, $n = 11$ to 12 cells to group. (**E**) Tet-On-D2R-IL3 spares quinpirole-induced inhibition of forskolin-induced accumulation of cAMP. LogIC_{50} is −9.78 for D2R-IL3 and −9.65 for D2R-IL3-Scr. $n = 3$ independent experiments per condition. (**F**) Top: Experimental time frame. Bottom left: Basal locomotor activity. Two-sided Student's *t* test, $t = 0.994$, df = 30, $P = 0.3282$, $n = 16$ mice per group. Bottom middle: Inhibition of D2R-NMDAR heteromerization blunts the development of locomotor sensitization. Three-way ANOVA: virus effect, $F_{1,192} = 1.984$; n.s., $P > 0.9999$; $n = 6$ to 8 mice per group. Bottom right: Sensitization scores of cocaine-treated mice injected with Tet-On-D2R-IL3-scr (black) or Tet-On-D2R-IL3 (green). One-sample Student's *t* test, $t = 3.258$, df = 7, #$P = 0.0139$ (cocaine IL3-Scr versus 0); $t = 1.782$, df = 7, $P > 0.05$ (cocaine IL3 versus 0). (**G**) Top: Experimental time frame. Bottom left: Impact of D2R-NMDAR heteromer inhibition on the maintenance of cocaine-evoked locomotor sensitization. Three-way ANOVA: virus effect, $F_{1,198} = 7.278$, *$P = 0.0330$, $n = 6$ mice per group. Bottom right: Sensitization scores of cocaine-treated mice injected with Tet-On-D2R-IL3-scr (black) or Tet-On-D2R-IL3 (green). One-sample Student's *t* test: $t = 4.170$, df = 5, ##$P = 0.0087$ (cocaine IL3-Scr versus 0); $t = 0.00$, df = 5, $P > 0.05$ (cocaine IL3 versus 0). Error bars denote SEMs.

distinct phases of long-term cocaine-evoked adaptations. We next examined whether receptor heteromerization also controls nondrug reward processing. We found that disrupting either heteromer subtype, using comparable conditions as for our studies with cocaine, failed to alter the reinforcing properties of food (Fig. 6), supporting a role of these heteromers in controlling the rewarding effects of cocaine but not a nondrug reward.

D2R-NMDAR heteromerization is increased in postmortem brain samples from individuals with psychostimulant use disorder despite decreased D2R expression

As evidenced above in mice, D2R-NMDAR heteromerization plays a cardinal role in the maintenance of cocaine's effects without affecting natural reward processing, which positions this heteromer subtype as a potential therapeutic target for drug addiction. We therefore investigated whether D2R-NMDAR heteromerization could be detected in human brain tissues and if it was modulated in subjects with a history of psychostimulant dependence.

PLA has recently been shown to be a suitable approach to detecting single proteins or receptor heteromers, including D2R–A2AR (adenosine A2 receptor), in human brain samples (*46*, *47*). We therefore performed single detection of D2R, the GluN2B subunit of NMDAR, and D2R-NMDAR heteromers in postmortem human samples from control subjects and matched individuals with a history of psychostimulant dependence. Although often suffering from a polydrug use disorder, these individuals were selected for their main dependence on psychostimulants and the presence of traces of psychostimulants in their blood at the time of death (table S1). From whole-slide images of caudate putamen samples, automated detection of PLA signal was performed from 25 high-magnification images per subjects randomly selected within the ventral part of the samples, which corresponds to the mouse NAc (fig. S6).

D2R single detection produced a dense punctate pattern in control subjects (Fig. 7A), as already reported (*46*). As expected, this signal was absent when PLA was performed in the absence of the primary antibody. We detected a significant decrease in relative

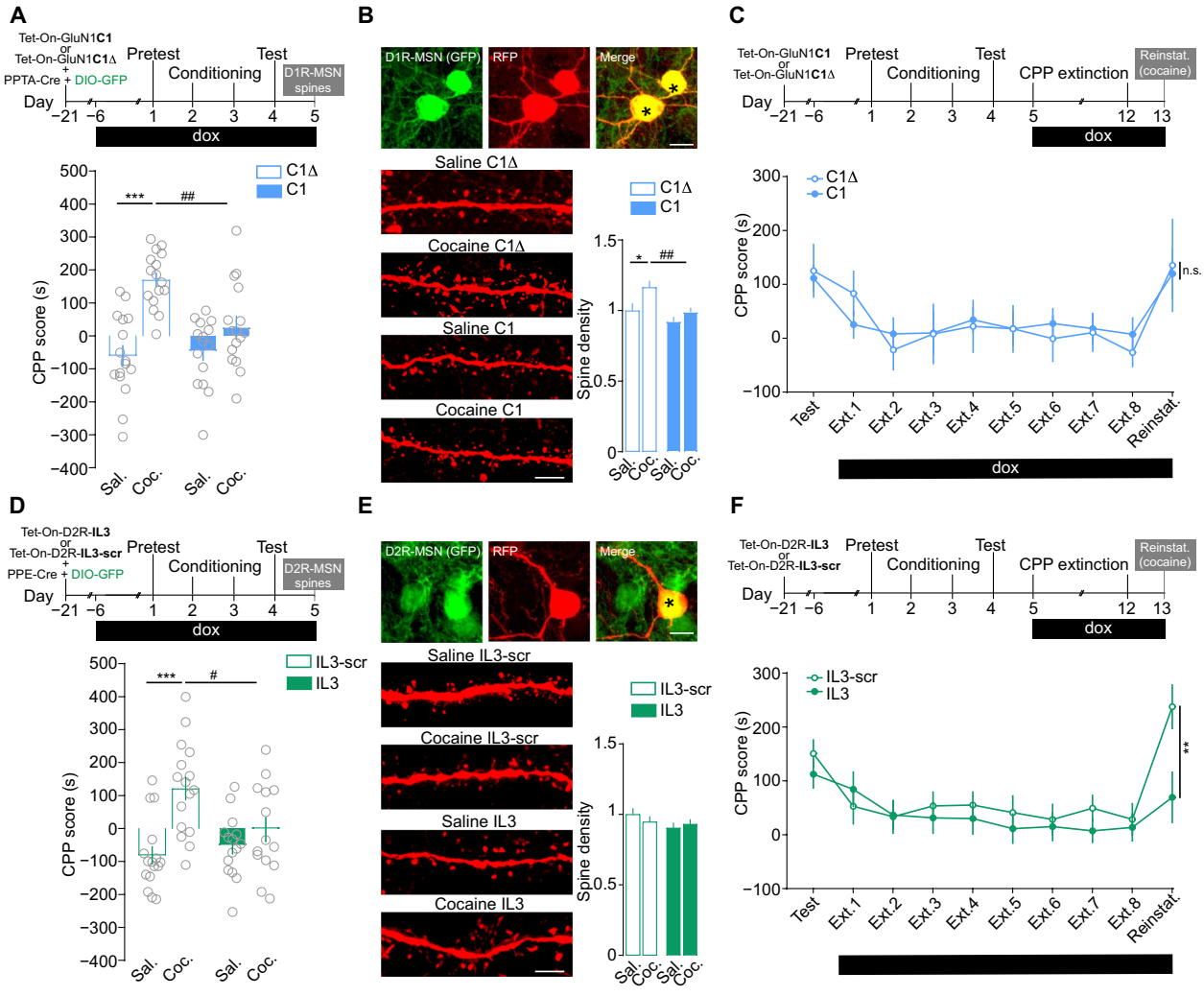

Fig. 5. Differential roles of D1R-NMDAR and D2R-NMDAR heteromerization in controlling the rewarding effects of cocaine. (**A**) Experimental time frame and CPP score upon inhibition of D1R-NMDAR heteromerization. Two-way ANOVA: virus effect, $F_{1,59} = 5.281$, $^{***}P < 0.0001$ and $^{\#\#}P = 0.0040$, $n = 15$ to 16 mice per group. (**B**) Top: Low magnification images of D1R-MSN (GFP^+; see fig. S3A) infected (RFP) shown by the asterisks. Scale bar, 10 μm. Bottom: High magnification of dendritic segments. Scale bar, 5 μm. Spine density analysis. Two-way ANOVA: virus effect, $F_{1,162} = 11.14$, $^{*}P = 0.0446$ and $^{\#\#}P = 0.0043$, $n = 27$ to 69 dendrites from six mice per group. (**C**) Experimental time frame to study the impact of D1R-NMDAR uncoupling on the extinction and cocaine-induced reinstatement (Reinstat.) of CPP. Two-way ANOVA: virus effect, $F_{1,24} = 0.004$, $P > 0.999$ (cocaine C1 versus cocaine C1Δ, CPP score on relapse day), $n = 10$ to 16 mice per group. (**D**) Same as for (A) upon inhibition of D2R-NMDAR heteromerization. Two-way ANOVA: virus effect, $F_{1,57} = 2.424$, $^{***}P < 0.0001$ and $^{\#}P = 0.0396$, $n = 14$ to 16 mice per group. (**E**) Top: Low-magnification images of D2R-MSN (GFP; see fig. S3B) infected (RFP) shown by the asterisk. Scale bar, 10 μm. Bottom: High-magnification of dendritic segments. Scale bar, 5 μm. Spine density analysis. Two-way ANOVA: virus effect, $F_{1,166} = 0.1268$; n.s., $P > 0.999$ (saline IL3-scr versus cocaine IL3-scr); $n = 30$ to 53 dendrites from six mice per group. (**F**) CPP score upon inhibition of D2R-NMDAR during CPP during extinction and cocaine-induced reinstatement. Two-way ANOVA: virus effect, $F_{1,31} = 0.899$, $^{**}P = 0.0018$ (cocaine IL3 versus cocaine IL3-scr CPP score on reinstatement day), $n = 16$ to 17 mice per group. Error bars denote SEMs.

D2R protein expression in samples from individuals with psychostimulant use disorder compared to control subjects (Fig. 7, A and B), consistent with the well-established decrease in striatal D2R availability reported in individuals suffering from psychostimulant misuse by positron emission tomography (PET) imaging (*33*, *48*–*51*). By contrast, the single detection of GluN2B subunits of NMDAR produced a dense PLA signal that was not different between both groups of subjects (Fig. 7, C and D). The double recognition of D2R-NMDAR proximity yielded a punctate signal in control subjects, which was undetectable when one of the two primary antibodies was omitted (Fig. 7E). In samples from individuals with psychostimulant use disorder, there was a trend toward an increase in D2R-NMDAR heteromers (Fig. 7F) despite the marked decrease in D2R levels. We therefore analyzed whether a correlation between individual receptor levels and D2R-NMDAR heteromerization could exist in individuals with a history of psychostimulant use disorder. We found a significant inverse correlation between these two parameters for D2R (Fig. 7G), but not GluN2B (Fig. 7H), suggesting that despite the lower levels of D2R expression, the remaining pool of D2R was preferentially involved in D2R-NMDAR heteromerization. In accordance, when normalizing the D2R-NMDAR PLA signal to D2R levels for each individual, we found a significant increase in relative D2R heteromerization with NMDAR in samples from people with psychostimulant use disorder when compared to controls (Fig. 7I).

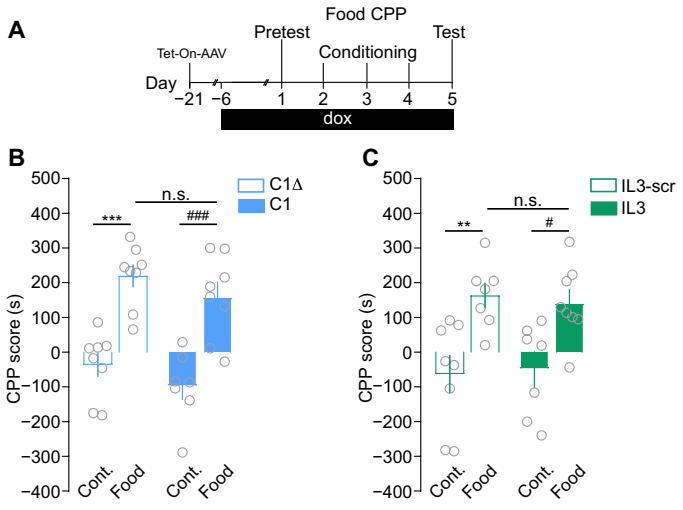

Fig. 6. Inhibiting D1R-NMDAR or D2R-NMDAR heteromerization does not alter CPP for food. (**A**) Experimental time frame to study the consequences of inhibition of heteromerization on the development of food-induced CPP. (**B**) Impact of inhibiting D1R-NMDAR heteromerization on the CPP score. Two-way ANOVA: virus effect, $F_{1,27} = 2.756$, $^{***}P = 0.0002$ (control C1Δ versus food C1Δ); $^{\#\#\#}P = 0.0002$ (control C1 versus food C1); n.s., $P > 0.999$ (food C1 versus food C1Δ); $n = 7$ to 8 mice per group. (**C**) Effect of inhibiting D2R-NMDAR heteromerization on the CPP score. Two-way ANOVA: virus effect $F_{1,26} = 0.007$, $^{**}P < 0.0098$ (control IL3-scr versus food IL3-scr); $^{\#}P = 0.0366$ (control IL3 versus food IL3); n.s., $P > 0.999$ (food IL3 versus food IL3-scr); $n = 7$ to 8 mice per group. Error bars denote SEMs.

Expression levels of D1R and GluN1 subunits of NMDAR, as well as D1R-NMDAR heteromerization, were also analyzed by PLA from the same human postmortem samples. Comparable levels of these two proteins were found in caudate putamen from control subjects and individuals with a history of psychostimulant misuse (fig. S7, A to D). By contrast, we observed decreased D1R-NMDAR heteromerization in individuals with psychostimulant use disorders (fig. S7, E to H). This latter result is reminiscent of the lower D1R-NMDAR interaction that we observed in mice after a 7-day period of abstinence in the NAc shell (see Fig. 2D).

To the best of our knowledge, these results provide the first direct evidence of a decreased D2R protein expression in the striatum of individuals with psychostimulant use disorder, which is associated with an increase in D2R-NMDAR heteromerization. Together with our interventional approach in mice, our data support D2R-NMDAR heteromers as therapeutic targets of potential interest in addiction.

DISCUSSION

Optogenetic studies have shown that distinct phases of drug-induced behavioral adaptations rely on DA-evoked synaptic adaptations at specific glutamate inputs onto MSN subpopulations (*13*–*15*, *52*, *53*). Nonetheless, the underlying molecular mechanisms remain poorly understood (*2*). This is an important issue because the identification of events responsible for such a detrimental interplay between DA and glutamate signaling may help in the development of innovative strategies with therapeutic potential. Here, we provide multiple lines of evidence, from mice to humans, that the heteromerization of glutamate NMDAR with D1R or D2R is modulated by psychostimulants and differentially controls the development and maintenance phases of cocaine-evoked long-term adaptations.

The focus on DAR and NMDAR heteromers as potential integrators of DA and glutamate inputs that may control drug-mediated adaptations stems from in vitro and ex vivo studies showing that such a direct physical interaction allows a reciprocal fine-tuning of the component receptors' functions (*23*, *27*). In particular, patch clamp recording from striatal slices showed that D1R-NMDAR and D2R-NMDAR interactions facilitate and inhibit NMDAR-mediated signaling upon DA increase, respectively (*31*, *32*). An appealing hypothesis would therefore be that, by linking DA to glutamate signaling in opposite ways, these heteromers could constitute molecular substrates for drugs of abuse to exert their differential effects on the activity of MSN subtypes, which has been proposed to underlie the switch from recreational drug consumption to addiction (*3*, *54*).

In agreement with this model, our PLA analysis showed that locomotor sensitization induced by repeated cocaine injections was associated with an increase in both heteromers in the NAc. We also found that this increased heteromerization requires DAR stimulation. While the PLA method cannot establish the direct physical contact of the two proteins or the stoichiometry of the complex, it does indicate that the proteins are in close molecular proximity (*34*). Nonetheless, previous studies have provided evidence for direct interactions between the D1R-NMDAR and D2R-NMDAR (*28*, *32*), and we find that our viral minigenes selectively decrease the PLA signals; we therefore interpret these PLA data as support for receptor heteromerization. While in-depth characterization of the molecular events responsible for this increased receptor interaction upon cocaine exposure is beyond the scope of this study, a possible explanation may lie in the observation that repeated cocaine exposure decreases PSD-95 expression in the NAc (*37*). PSD-95 is a known endogenous inhibitor of D1R-NMDAR interaction (*38*) that also binds to D2R (*55*) and the C-terminal end of GluN2B subunits of NMDAR (*56*). Although the PLA approach is able to provide a snapshot of the impact of cocaine on receptor heteromerization in situ in their native environment (*31*, *34*, *57*), future work is needed to investigate whether heteromerization of DAR and NMDAR is an input-specific process and whether it relies on the modulation of receptor surface expression and/or dynamics.

The development of the sensitizing effects of cocaine has been previously causally linked to the potentiation of glutamate transmission at cortical projections onto D1R-MSN of the NAc (*13*). Since we observed that preventing D1R-NMDAR heteromerization reversed both alterations in A/N ratio and the development of behavioral sensitization while sparing the function of individual component receptors [see (*31*)], our results suggest that D1R-NMDAR heteromers are key molecular platforms for the development of cocaine-induced long-term adaptations. In contrast, disrupting D1R-NMDAR interaction during abstinence from cocaine did not disrupt maintenance of the sensitized state, supporting a preferential role of this heteromer subtype in the initial phases of cocaine-mediated adaptations. In agreement with this hypothesis, we observed that preventing D1R-NMDAR heteromerization during CPP conditioning also blocked the development of the rewarding effects of cocaine but failed to alter the extinction and reinstatement phases. This critical time window of D1R-NMDAR heteromer function restricted to the early developmental phase of cocaine-evoked adaptations agrees with our observation that cocaine-induced D1R-NMDAR heteromerization is a transient mechanism that does not outlast a 7-day abstinence period. Instead, the temporally controlled disruption of D2R-NMDAR

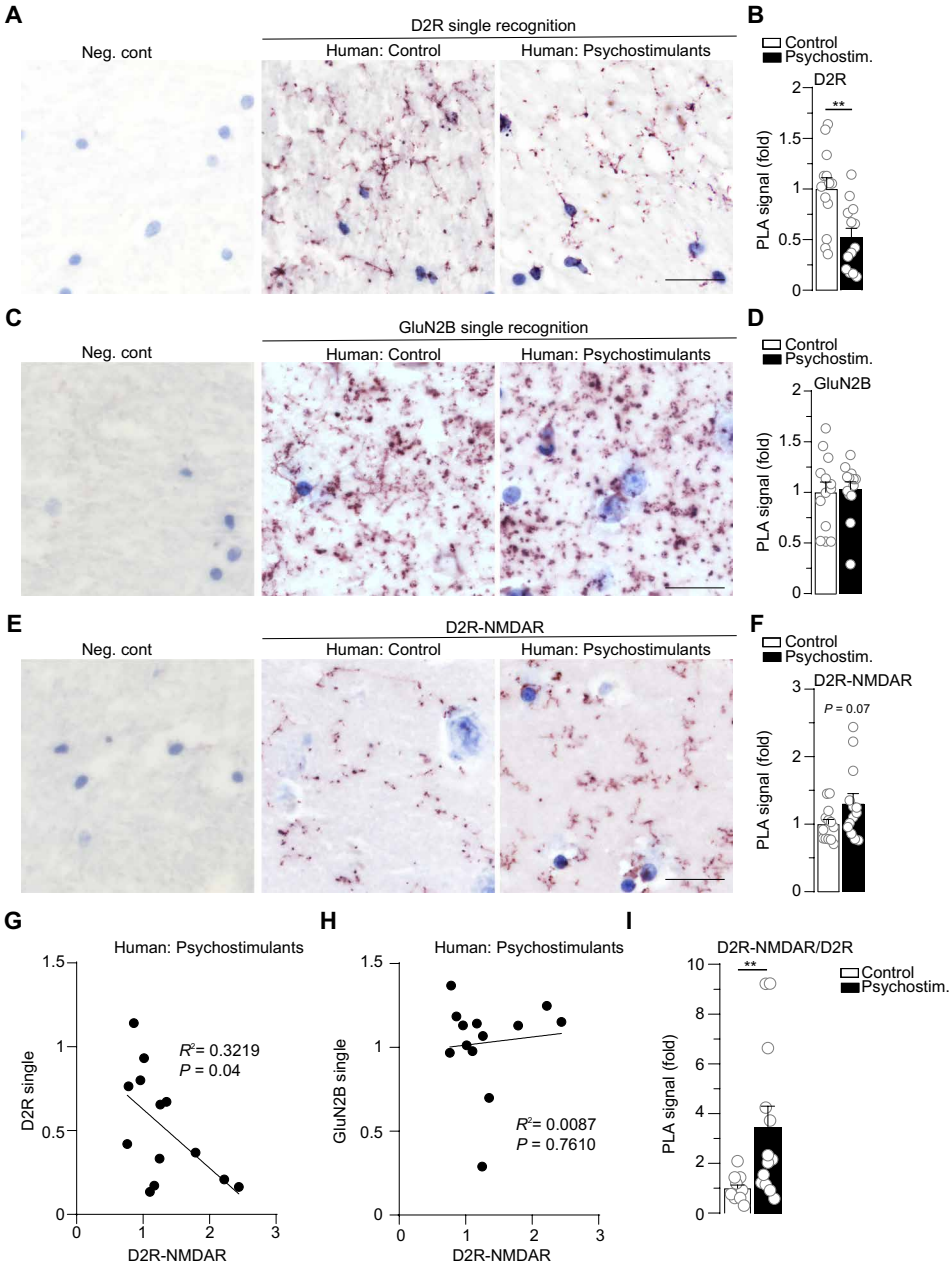

Fig. 7. D2R-NMDAR heteromerization is increased in postmortem brain samples from individuals with psychostimulant use disorder despite decreased D2R expression. (**A**) Representative images of D2R single recognition by PLA in human control subjects (Human: Control) or individuals having suffered from psychostimulant use disorder (Human: Psychostimulants) and negative control, in which the primary antibody is omitted (left; Neg. cont; see fig. S6). (**B**) Quantifications of D2R single PLA signal represented as fold decrease compared to control subjects. Two-sided Student's *t* test: $t = 3.331$ df = 24, $^{**}P = 0.0028$, $n = 13$ subjects per group. (**C**) Example images of GluN2B subunit of NMDAR single detection and Neg. cont. (**D**) Quantifications of Glu2NB PLA signal. Two-sided Student's *t* test, $t = 0.224$ df = 24, $P = 0.8243$, $n = 13$ subjects per group. (**E**) Illustrative images of D2R-NMDAR heteromer detection by PLA and Neg. cont (GluN2B antibody omitted). (**F**) Quantifications of D2R-NMDAR PLA signal. Two-sided Student's *t* test: $t = 1.868$ df = 24, $P = 0.074$, $n = 13$ subjects per group. (**G**) Pearson correlation between D2R expression levels and D2R-NMDAR heteromerization for each sample from all individuals having suffered from psychostimulant use disorder. $R^2 = 0.3219$, $P = 0.0432$. (**H**) Same as in (G) for the Pearson correlation between GluN2B expression levels and D2R-NMDAR. $R^2 = 0.0087$, $P = 0.761$. (**I**) Quantifications of D2R-NMDAR PLA signal normalized to D2R expression levels for each subject. Two-sided Student's *t* test, $t = 2.882$ df = 24, $^{**}P = 0.0082$, $n = 13$ subjects per group. Scale bars, 25 μm (A, C, and E). Error bars denote SEMs.

heteromers revealed their important role in controlling both the development and maintenance of the sensitizing and rewarding effects of cocaine. In agreement with these findings, we found that D2R-NMDAR heteromerization persisted through abstinence from cocaine. Moreover, this persistent heteromerization was specifically observed in the NAc core, which has been identified as a common output structure of neuronal circuits involved in both cue- and drug-induced reinstatement (*58*). Since the optogenetic activation of D2R-MSNs in the NAc has been shown to preserve cocaine-induced locomotor sensitization but to blunt its expression after abstinence

(*59*), our results support a model by which inhibiting endogenous D2R-NMDAR interaction during abstinence hinders the persistence of cocaine-evoked responses by potentiating D2R-MSN activity. Since D2R-GluN2B heteromerization has been shown to mediate the D2R agonist–induced inhibition of NMDAR functions ex vivo (*32*), we reasoned that disrupting D2R-NMDAR interaction, by preventing the inhibitory effect of DA on NMDAR signaling, could artificially activate signaling pathways and transcription in D2R-MSN. To test this hypothesis, we studied expression levels of ΔFosB in D2R-MSN upon blockade of D2R-NMDAR interaction. ΔFosB expression has been used here as a reporter gene for the activation of signaling pathways and gene expression. We found that disrupting D2R-NMDAR heteromerization during an abstinence period was associated with an increase in ΔFosB in D2R-MSN upon reexposure to the drug. Because ΔFosB overexpression in D2R-MSN has been shown not to affect behavioral responses to cocaine (*42*–*44*), the increased ΔFosB expression in D2R-MSN that we observed upon blockade of D2R-NMDAR heteromerization is unlikely responsible for the alteration of the persistence of the sensitization and rewarding effects of cocaine CPP but rather reflects the ability of D2R-NMDAR to modulate cocaine-induced signaling in D2R-MSN. Nevertheless, our results strongly support that D2R-NMDAR heteromerization is a key molecular mechanism triggered by cocaine that alter signaling in D2R-MSN and contributes to the persistence of cocaine-evoked adaptations.

Notably, there exists another epitope within the IL3 of D2R ($_{217}$RRRRKRR$_{222}$) that is involved in the interaction of D2R with A2AR (*60*). Furthermore, cocaine self-administration has been shown to trigger an increase in D2R-A2AR heteromerization in the NAc (*61*), which plays a functional role at the behavioral level (*62*). On the basis of these findings and as opposed to previous work targeting D2R-NMDAR heteromerization (*32*), we designed AAV-Tet-On-D2R-IL3 to express a fragment of D2R-IL3 that does not include the D2R-IL3 fragment responsible for D2R-A2AR interaction. This suggests that the inhibition of the development and persistence of cocaine-evoked adaptations that we observed are likely due to a direct inhibitory effect of AAV-Tet-On-D2R-IL3 on D2R-NMDAR interaction. However, because D2R binds to both NMDAR and A2AR, we cannot exclude the possibility that disrupting D2R-NMDAR interaction may indirectly modulate D2R-A2AR heteromerization. Regardless, our results strongly support D2R-NMDAR heteromers as molecular targets with a potential therapeutic value.

Direct manipulations of MSN activity have clearly revealed that D1R-MSN and D2R-MSN activation facilitates and blunts the development and maintenance phases of psychostimulant-induced behavioral adaptations, respectively (*2*). Notably, our findings that D1R-NMDAR and D2R-NMDAR heteromerization controls distinct phases of cocaine-induced locomotor sensitization highlight that these receptor complexes mediate discrete properties of MSN subpopulations and play complementary roles to mediate the full panel of cocaine-induced adaptations. In further support of specific functions of DA and glutamate receptor heteromers, we established that their roles in shaping reward processing depend on the nature of the reward since the disruption of either receptor heteromer blocked the development of cocaine-induced CPP but spared food-mediated CPP. Although the mechanisms underlying this selectivity to drug reward remain to be established, our findings suggest that targeting DA-glutamate receptor heteromers has the potential to preferentially alleviate pathological adaptations induced by drugs of abuse. In particular, the role for D2R-NMDAR heteromerization in maintaining cocaine-induced adaptations, combined with its lack of implication in reward processing to a natural reinforcer, suggests that D2R-NMDAR heteromers are targets of choice from a translational standpoint. This first led us to investigate whether this heteromer subtype could be detected in postmortem human samples and modulated in subjects with a history of psychostimulant consumption.

Our PLA analysis revealed a strong reduction of D2R protein levels in the NAc of individuals with psychostimulant use disorder. This first observation of a decreased D2R protein expression in postmortem brain samples from individuals having suffered from psychostimulant misuse is consistent with the down-regulation of D2R mRNA levels that has been described after long-term cocaine exposure in rats (*63*). This finding could also partly account for the decrease in D2R binding readily observed with PET imaging in the striatum of subjects with psychostimulant use disorder (*33*, *48*–*51*). Despite this down-regulation of D2R protein, the proportion of D2R forming heteromers with GluN2B subunits of NMDAR was threefold higher in samples from subjects with a history of psychostimulant misuse compared to control subjects. Notably, individuals with psychostimulant use disorder bearing the lowest D2R expression displayed the highest density of D2R-NMDAR. This raises questions regarding the underlying molecular mechanism of D2R-NMDAR heteromer formation in response to psychostimulant exposure in human. On the basis of our findings in mice that cocaine-induced D2R-NMDAR heteromerization depends on D2R stimulation, it is tempting to speculate that repeated increases of phasic DA levels resulting from recurrent psychostimulant consumption could be responsible for the higher D2R-NMDAR receptor proximity. By contrast, we observed a decreased D1R-NMDAR heteromerization in subjects with psychostimulant use disorder. This decrease might be linked to the transient nature of cocaine-induced D1R-NMDAR heteromerization that we identified in mice treated with cocaine and subjected to an abstinence period. In the case of human samples, although the history of drug use disorder was accurately characterized, we do not have information about when these individuals last consumed psychostimulants. Therefore, the decrease in D1R-NMDAR heteromers that we measured in subjects with a history of psychostimulant use disorder may result from the delay between the last drug consumption and the time of death. By contrast, the increase in D2R-NMDAR heteromerization that we observed in the ventral striatum of subjects with psychostimulant use disorder agrees with our finding that cocaine-induced D2R-NMDAR heteromerization in the NAc core of mice outlasts a 7-day abstinence period. Nonetheless, the increased D2R-NMDAR heteromerization that we observed in human samples from individuals with psychostimulant use disorder, together with interventional approaches in mice, emphasizes their roles in the persistence of cocaine's behavioral effects. These findings constitute an important breakthrough in our understanding of the molecular bases of cocaine-induced adaptations and highlight the potential benefit of targeting D2R-NMDAR heteromerization not only in the field of addiction but also potentially for multiple neuropsychiatric disorders associated with an imbalance of DA and glutamate transmission.

MATERIALS AND METHODS

Animals

Six-week-old C57BL/6J male mice were purchased from Janvier Labs (Le Genest-Saint-Isle, France). The animals were housed four per cage, in a 12-hour light/12-hour dark cycle, under stable temperature (22°C) and humidity (60%) conditions with ad libitum

access to food and water. They were acclimatized to the animal facility for at least 1 week. All experiments were carried out in accordance with the standard ethical guidelines [European Community Council Directive on the Care and Use of Laboratory Animals (86/609/EEC) and the French National Committee (2010/63)].

Drugs

Drugs were administrated intraperitoneally in a volume of 10 ml/kg. Cocaine hydrochloride (Sigma-Aldrich, St. Louis, MO) was dissolved in a saline solution [0.9% (w/v) NaCl].

9-*tert*-butyl dox hydrochloride (9TB-dox; tebu-bio, Le Perray-en-Yvelines, France) was dissolved in a saline solution containing dimethyl sulfoxide (DMSO; 5%) and Tween 20 (5%). SCH23390 (0.25 mg/kg) or eticlopride (0.5 mg/kg) dissolved in a saline solution [0.9% (w/v) NaCl] were administered 30 min before the challenge cocaine injection.

Viral constructions

All AAV recombinant genomes were packaged in serotype 9 capsids. AAV-Tet-On-GluN1C1 bicistronically expresses the fluorescent reporter protein RFP and the C1 cassette of the GluN1 subunit ($_{864}$DRKSGRAEPDPKKKATFRAITSTLASSFKRRRSSKDT$_{900}$) upon dox treatment. The related control virus AAV-Tet-On-GluN1C1Δ expresses a truncated version of C1 that is deleted from a stretch of nine positively charged amino acids ($_{890}$SFKRRRSSK$_{898}$), which are required for D1R-GluN1 interaction (*54*). The AAV-Tet-On-D2R-IL3 encodes a sequence of the IL3 of the D2R ($_{225}$TKRSSRAFRA$_{234}$) interacting with GluN2B. The control AAV-Tet-On-D2R-scr expresses a scrambled sequence (KFARRTSASR) of the D2R-IL3 (full AAV sequences are available upon request). All Tet-On AAV were injected bilaterally by infusing 0.7 µl of a solution at 5.10^{13} viral genomes/ml per hemisphere for the NAc (2 µl for the dorsal striatum). The AAV-PPTA-Cre and AAV-PPE-Cre contain an expression cassette consisting of the Cre recombinase driven by the promoter of the PPTA gene or the PPE gene, which are specifically expressed in D1R-MSN and D2R-MSN, respectively (see fig. S3) (*7*, *39*, *40*). AAV PPTA-Cre or AAV-PPE-Cre were coinjected with the AAV-pCAG-DIO-eGFP-Woodchuck hepatitis virus Post-translational Regulatory Element (WPRE) (Upenn) expressing flexed eGFP under the cytomegalovirus/actin hybrid promoter (CAG). All viruses were diluted in phosphate-buffered saline (PBS) with 0.001% pluronic.

Stereotaxic injections

Mice were anesthetized with ketamine (150 mg/kg) and xylazine (10 mg/kg) and placed on a stereotaxic apparatus (David Kopf Instruments, Tujunga, CA, USA). Craniotomies were realized using the following coordinates: 1.7 mm rostral to the bregma, 1.2 mm lateral to midline, and 4.6 mm ventral to the skull surface to target the NAc and 1 mm rostral to the bregma, 1.8 mm lateral to midline, and 3.25 mm ventral to the skull surface for the dorsal striatum. Viral injections were performed bilaterally at a rate of 0.15 µl/min using a 10-µl syringe (Hamilton 1700 series, PHYMEP, Paris, France) with a 200-µm gauge needle (PHYMEP, Paris, France) mounted on a microinfusion pump (Harvard Apparatus, Holliston, MA). After the injection, the needle was left in place for an additional 8 min to avoid backflow.

Dox treatments

Three weeks after stereotaxic injections of Tet-On-AAV, the expression of the constructs was triggered by daily intraperitoneal injection of 9TB-dox (10 mg/kg) for 4 days. To maintain expression, mice were then supplemented with a mix containing dox HCl (2 mg/ml), 9TB-dox HCl (80 µg/ml), and sucrose (1%) added in drinking water.

Behavioral testing

All behavioral tests were conducted during the light phase (8:00 to 19:00). Animals were randomly assigned to the saline or cocaine groups after viral injection. Before behavioral testing, mice were handled daily for 7 days in the experiment room. All mice were perfused with 4% (w/v) paraformaldehyde (PFA) 24 hours after behavior to systematically verify the accuracy of stereotaxic injections and expression of the RFP reporter protein. Mice that did not meet quality criterion (i.e., nonbilateral expression, off-target diffusion, excessive backflow, or low RFP expression) were discarded from the study.

Locomotor activity and cocaine psychomotor sensitization

Locomotor activity was measured in a low-luminosity environment inside a circular corridor (Immetronic, Pessac, France) containing four infrared beams placed at each 90° angle. Locomotor activity was expressed as a cumulative count of crossings between quarters of the corridor for the indicated time. Mice were treated with dox 7 days before and until the end of the experiment. Mice were habituated to the test apparatus for 3 days; basal locomotor activity was recorded on the third day of habituation. Cocaine sensitization experiments consisted of five daily 90 min sessions during which spontaneous activity was recorded for 30 min before saline or cocaine (15 mg/kg) injections, and locomotor activity was then measured for 60 min after injections. To study the consequences of uncoupling DAR from NMDAR on the maintenance of cocaine-induced locomotor sensitization, mice were treated for five consecutive days with saline or cocaine in the absence of dox. After the last injections, mice were supplemented with dox during an abstinence period, followed by a challenge injection of saline or cocaine. To analyze whether cocaine-treated groups injected with Tet-On viruses developed significant behavioral sensitization, we calculated a sensitization score defined as the locomotor at day 5 minus locomotion at day 1. Similarly, to assess the impact of Tet-On viruses on the maintenance of locomotor sensitization in the cocaine-treated groups, we calculated a sensitization score corresponding to the locomotion at day 12 (cocaine challenge) minus the locomotion at day 5. One-sample Student's *t* tests were used to determine whether sensitization scores obtained in each group were significantly different from 0, corresponding to the sensitization score of animals displaying an absence of sensitization.

Cocaine CPP

To study the impact of DAR-NMDAR heteromerization on the development of CPP, mice were treated with dox for 7 days before and until the end of the experiment. The CPP was performed in a two-compartment Plexiglas Y-maze apparatus (Imetronic). Each compartment contains different visual cues and floor textures for which mice did not show any preference on average before conditioning. All sessions lasted 20 min. On day 1, mice were placed in the center of the apparatus and allowed to explore both compartments freely. Time spent in each compartment was automatically recorded. Mice spending more than 70% of the time in one compartment were excluded. On day 2, to avoid any initial preference bias, mice were randomly assigned to one or the other compartment

for each group. Mice were injected with saline and placed immediately in the assigned closed compartment for 20 min. After 1 hour, mice were injected with saline or cocaine and placed in the other closed compartment. This was repeated on day 3. The test was performed on day 4, during which mice had a free access to both chambers. The CPP score was calculated as the difference between the time spent in the cocaine-paired chamber during day 4 and the time spent in this compartment on day 1. CPP extinction and maintenance experiments were performed on the cocaine groups of mice injected with Tet-On-AAV that developed a preference for the cocaine-paired chamber in the absence of dox. Mice were then treated with dox until the behavioral assessment. For the extinction phase, mice were injected with saline and put back in the apparatus with free access to both compartments for 20 min daily for 8 days. On the ninth day, mice were injected with cocaine and allowed to explore both compartments.

For palatable food-induced CPP, mice were food-deprived to 90% of initial ad libitum weight and treated with dox 7 days before and during behavioral assessment. Experiments were performed in the same apparatus and conditions as for cocaine-induced CPP with the following modifications: On day 2, after random group assignment, mice were placed immediately in the assigned closed compartment containing chocolate crisps (Chocapic, Nestlé, Vevey, Switzerland) or nothing for 20 min. After 1 hour, mice were placed in the other closed compartment. This was repeated on days 3 and 4. The test was performed on day 5.

Mouse tissue preparation

Mice were anesthetized with an intraperitoneal injection of Euthasol (100 mg/kg; Le Vet, Oudewater, The Netherlands) and perfused transcardially with 0.1 M Na_2HPO_4/ Na_2HPO_4 (pH 7.5) containing 4% PFA at 4°C, delivered with a peristaltic pump at 20 ml/min for 5 min. Brains were then extracted, postfixed overnight in 4% PFA, and stored at 4°C. Coronal sections (30 μm in thickness) were performed with a vibratome (Leica, Nussloch, Germany) and kept at −20°C in a cryoprotective solution containing 30% (v/v) ethylene glycol, 30% (v/v) glycerol, and 0.1 M PBS.

Immunohistochemistry

On day 1, free-floating sections were rinsed three times for 5 min in tris-buffered saline [TBS; 0.9% NaCl and 0.1 M tris base (pH 7.5)]. Sections were then incubated in blocking solution containing 3% normal goat serum, 0.2% Triton X-100 (Sigma-Aldrich), and 50 mM NaF for 2 hours at room temperature (RT) before overnight 4°C incubation with primary antibodies (see Table 1) diluted in the blocking buffer. On day 2, after three 10-min rinses in TBS, sections were incubated for 90 min with secondary antibodies (see Table 1). The anti-FosB antibody recognizes full-length FosB and ΔFosB, but at the time point studied (24 hours after cocaine), all FosB-immunoreactive protein represents ΔFosB (*43*). After three 5-min rinses in TBS, sections were incubated for 5 min with Hoechst (Invitrogen) for nuclei counterstaining. Three 5-min TBS and two tris buffer [0.1 M tris base (pH 7.5)] washes were performed before sections were mounted in ProLong Gold (Invitrogen).

Immunoblotting

Mice were euthanized by decapitation, and their heads were immediately snap-frozen in liquid nitrogen. Microdiscs of NAc were punched out using disposable biopsy punches (1 mm in diameter) (Kai Medical) and stored in individual tubes at −80°C. Microdiscs were then homogenized by sonication in a lysis solution containing 50 mM tris HCl, 2% SDS, and 0.5 M urea diluted in water. Protein concentrations were determined using a Bicinchoninic Acid (BCA) assay kit (Pierce, Rockford, IL). A fixed amount of protein (30 μg per lane) was separated by SDS–polyacrylamide gel electrophoresis (12%) before electrophoretic transfer onto nitrocellulose membranes. Membranes were incubated for 1 hour at RT in a blocking solution containing TBS with 0.1% Tween and 5% nonfat dry milk. Membranes were incubated at 4°C overnight with primary antibodies (see Table 1). Membranes were then washed three times in TBS-Tween and then incubated for 1 hour at RT with secondary antibodies (see Table 1) coupled to horseradish peroxidase (HRP). Immunoreactive bands were detected by chemiluminescent detection (ECL kit, GE Healthcare), and images were acquired using the ImageQuant LAS 4000 (GE Healthcare Life Science). The densitometry of immunoreactive bands was quantified using ImageJ and normalized to the loading control.

Human brain samples

Brain samples from individuals with a history of substance dependence, with toxicological evidence of current psychostimulant use, and from matched healthy controls (n = 13 per group; table S1) were provided by the Suicide section of the Douglas-Bell Canada Brain Bank (DBCBB). Brains were donated to the DBCBB by familial consent through the Quebec Coroner's Office, which ascertained the cause of death. Two months after death, psychological autopsies with next-of-kin were conducted, as previously described (*64*).

Dissections of ventral striatum were performed with the guidance of a human brain atlas (*65*) on 0.5-cm-thick formalin-fixed coronal brain sections at an anatomical level equivalent to plate 15 of this atlas (−7.5 mm from the center of the anterior commissure). Tissue was extracted rostral to the anterior commissure and ventral to the tip of the anterior limb of internal capsule and fixed by immersion in formalin until paraffin embedding. The latter was completed using a Leica ASP200S automated processor. Tissue blocks were dehydrated in increasing gradients of alcohol (70, 95, and 3 × 100%) for 1.5 hours each, followed by clearing in three changes of 100% xylene (2 hours and 2 × 1.5 hours). The samples were then infiltrated in three changes of molten paraffin, 3 hours each before embedding. Slices of 6 μm in thickness were then prepared with microtome at the histology facility of the ICM Institute (Paris).

Proximity ligation assay

PLA on mouse brain sections (30 μm in thickness) was performed in 48-well plates according to the manufacturer's instructions for free-floating sections. PLA on human postmortem paraffin-embedded tissue was performed on sections mounted on Superfrost plus slides (Thermo Fisher Scientific). Human caudate putamen sections (6 μm in thickness) were deparaffinized in xylene, rehydrated in graded ethanol series, and washed briefly in TBS. For antigen retrieval, sections were boiled for 6 min in sodium citrate buffer (10 mM; pH 6). For bright-field PLA, sections were incubated for 30 min at RT in TBS containing 1% H_2O_2 to block endogenous peroxidase. After three 5-min rinses with TBS containing 0.1% Triton X-100, sections were incubated for 1 hour at RT with blocking buffer (Duolink blocking buffer for PLA) and then with primary antibodies (see Table 1) diluted in the Duolink antibody dilution buffer overnight at 4°C. Anti-rat PLA plus and minus probes were made using the

Table 1. List of primary and secondary antibodies. IHC, immunohistochemistry; WB, Western blot; IgG, immunoglobulin G.

Primary antibody	Reference	Application	Dilution	Secondary antibody	Antibody origin	Dilution
Rabbit polyclonal to phospho-GluN2B (Y1472)	Abcam, Cambridge, UK; ref.: ab3856	IHC	1:200	Alexa Fluor 488 goat anti-rabbit IgG	Thermo Fisher Scientific, Waltham USA, ref.: A11034	1:500
Rabbit monoclonal to phospho-Erk1/2 (Thr^{202}/Tyr^{204})	Cell Signaling Technology, Danvers, USA; ref.: 4370S	IHC	1:400	Alexa Fluor 488 goat anti-rabbit IgG	Thermo Fisher Scientific, ref.: A11034	1:500
Rat monoclonal to D1R	Sigma-Aldrich, St Louis, USA; ref.: D2944	PLA	Dual PLA: 1:200;single PLA: 1:200			
		WB	1:500	ECL goat anti-rat IgG, HRP-linked	GE Healthcare, Chicago, USA; ref.: NA935	1:5000
Rabbit polyclonal to NMDAR1	Abcam, Cambridge, UK; ref.: ab17345	PLA	Dual PLA: 1:200; single PLA: 1:400			
Rabbit polyclonal to D2R	Millipore, Burlington, USA; ref.: ABN462	PLA	Dual PLA: 1:200; single PLA: 1:400			
		WB	1:500	WB: ECL goat anti-rabbit IgG, HRP-linked	GE Healthcare; ref.: NA934	1:5000
Mouse monoclonal to NMDAR2B NT	Millipore; ref.: MAB5782	PLA	Dual PLA: 1:200; single PLA: 1:500			
		WB	1:500	WB: ECL goat anti-mouse IgG, HRP-linked	GE Healthcare, Chicago, USA; ref.: NA931	1:5000
Mouse monoclonal to NMDAR1 CT	Millipore; ref.: 05-432	WB	WB: 1:200	WB: ECL goat anti-mouse IgG, HRP-linked	GE Healthcare; ref.: NA931	1:5000
Rabbit polyclonal to Fos B	Santa Cruz Biotechnology; ref: sc-48	IHC	1:500	Cy5 goat anti-rabbit IgG	Jackson ImmunoResearch; ref: AB_2338013	1:1000

PLA Probemaker Kit (Sigma-Aldrich) with a goat anti-rat immunoglobulin G antibody (Jackson ImmunoResearch) according to the manufacturer's instructions. Immunofluorescent PLA and the remaining procedures for bright-field PLA were performed as previously described (*31*). For bright-field PLA, nuclei were counterstained using the Duolink nuclear stain. In this study, we used both single-recognition PLA, using only one primary antibody to detect single antigen, and dual recognition to detect DAR-NMDAR complexes using two primary antibodies.

Image acquisition and analysis

For immunochemistry and fluorescent PLA staining, images were taken with a confocal laser scanning microscope (SP5, Leica) using a 20× and a 63× objective (oil immersion; Leica) respectively. The pinhole was set to 1 Airy unit; excitation wavelength and emission range were 495 nm and 500 to 550 nm for green PLA signal, 488 nm and 500 to 550 nm for Alexa Fluor 488, and 590 to 650 nm for RFP. Laser intensity and detector gain were constant for all image acquisitions. Images were acquired in a range of 5 μm with a *z*-step of 0.2 μm. Conditions were run in duplicate, and quantifications were made from at least four images per condition. Four mice were used for each condition. Maximum projection images were analyzed using ImageJ [National Institutes of Health (NIH), Bethesda, MD].

For PLA image quantification, ImageJ was used to construct a mask from RFP-positive cells. The mask was then fused with the PLA signal–containing channel using the image multiply function. The PLA punctate signal was quantified on the resulting image in ICY using the spot detector function (detector: scale, 3:65; filtering: minimum size, 6; maximum size, 30); these parameters were chosen manually from random images to obtain optimal signal-to-noise ratio and minimal false positive in images from negative control conditions. RFP-positive cells showing at least one PLA puncta for one or the other heteromer subtypes were included, as this allowed us to identify the MSN subtype analyzed (D1R-MSN versus D2R-MSN). RFP-positive cells that did not present any D1R-GluN1 or D2R-GluN2B PLA signal were discarded.

Mouse bright-field PLA images were taken using a microscope (Leica, DM4000) with a 63× objective. A minimum of six random fields per structure per mice were taken.

For human bright-field PLA, whole-slide images were taken using a Zeiss Axioscan with a 40× magnification and *z*-stack with a 1-μm step interval. Whole-slide scanned images were visualized with ZEN Blue edition lite software (Zeiss, version 3.1). Twenty-five regions of interest of 500 μm by 500 μm were generated randomly in the NAc and were exported as TIFF files using the image export plugin. The *z*-stack with the maximum number of PLA signal in the focus was chosen for each image.

Human and mouse bright-field PLA images were analyzed using an ImageJ homemade macro that uses the Find Maxima tool to detect the PLA punctate with prominence set to >40. Results are represented as the mean PLA signal density per field of views. For quantification of immunohistochemistry experiments, immunoreactive cells were analyzed using ImageJ, considering the cells with immunofluorescence above a fixed threshold.

Neuronal survival

Neuronal survival was quantified manually on the basis of Hoechst-counterstained nuclei. Survival was defined as the percentage of viable neurons exhibiting large, uniform nuclei and even distribution of Hoechst among RFP-positive cells over RFP-positive cells classified as apoptotic on the basis of, at least, two of the following criteria: condensed nuclei, single chromatin clump, small nuclei size, noncircular nuclei shape, and increased Hoechst intensity.

Spine density analysis

Twenty-four hours after the CPP paradigm, mice were perfused and brains were sliced as described above. Dendrite spine analysis was performed on RFP-positive dendrites from D1R-MSN and D2R-MSN identified on the basis of the presence of GFP driven by the coinjection of AAV-PPTA-Cre/AAV-pCAG-DIO-eGFP or AAV-PPE-Cre/pCAG-DIO-eGFP, respectively. Image stacks were taken using a confocal laser scanning microscope (SP5, Leica). For analysis of D1R-MSN, images were collected through a 63× objective with a pixel size of 65 nm and a *z*-step of 200 nm. For D2R-MSN, images were collected through a 40× objective with a pixel size of 95 nm and a *z*-step of 300 nm. The excitation wavelength was 488 nm for GFP and 561 nm for RFP, with an emission range of 500 to 550 nm and 570 to 650 nm, respectively. Images were acquired in sequential mode with a Hybrid detector (Leica). Deconvolution with experimental point spread function from fluorescent beads using a maximum likelihood estimation algorithm was performed with Huygens software (Scientific Volume Imaging). NeuronStudio software was used to reconstruct the dendrite and detect dendritic spines with manual correction.

Patch clamp recordings

Mice were anesthetized [ketamine (150 mg/kg)/xylazine (10 mg/kg)] and transcardially perfused with artificial cerebrospinal fluid (aCSF) for slice preparation. Coronal 250-μm slices containing the NAc were obtained in bubbled ice-cold 95% O_2/5% CO_2 aCSF containing 2.5 mM KCl, 1.25 mM NaH_2PO_4, 10 mM $MgSO_4$, 0.5 mM $CaCl_2$, 11 mM glucose, 234 mM sucrose, and 26 mM $NaHCO_3$, using a HM650V vibratome (Microm, France). Slices were then incubated in aCSF containing 119 mM NaCl, 2.5 mM KCl, 1.25 mM NaH_2PO_4, 1.3 mM $MgSO_4$, 2.5 mM $CaCl_2$, 26 mM $NaHCO_3$, and 11 mM glucose, at 37°C for 1 hour, and then kept at RT. Slices were transferred and kept at 31°C in a recording chamber superfused with aCSF (2 ml/min) in the continuous presence of 50 μM picrotoxin (dissolved in DMSO; Sigma-Aldrich, France) to block GABAergic transmission. Neurons were visualized by combined epifluorescent and infrared/differential interference contrast visualization using an Olympus upright microscope holding 5× and 40× objectives. Whole-cell voltage clamp recording techniques were used to measure synaptic responses using a MultiClamp 700B (Molecular Devices, Sunnyvale, CA). Signals were collected and stored using a Digidata 1440A converter and pCLAMP 10.2 software (Molecular Devices, CA). AMPAR/NMDAR ratio was assessed using an internal solution containing 130 mM CsCl, 4 mM NaCl, 2 mM $MgCl_2$, 1.1 mM EGTA, 5 mM Hepes, 2 mM Na_2 adenosine 5′-triphosphate, 5 mM sodium creatine phosphate, 0.6 mM Na_3 guanosine 5′-triphosphate, and 0.1 mM spermine. Synaptic currents were evoked by stimuli (60 μs) at 0.1 Hz through a glass pipette placed 200 μm from the patched neurons. Evoked EPSCs were obtained at $V = +40$ mV in the absence and presence of the AMPAR antagonist 6,7-dinitroquinoxaline-2,3-dione. In all cases, 30 consecutive EPSCs were averaged, and offline analyses were performed using Clampfit 10.2 (Axon Instruments, USA) and Prism (GraphPad, USA). Pharmacologically isolated EPSC NMDAR decay time, recorded from cells voltage clamped at +40 mV, was fitted with a double exponential function, using Clampfit software, to calculate both slow and fast decay time constants, τ_{fast} and τ_{slow}, respectively. The weighted time constant ($\tau_{weighted}$) was calculated using the relative contribution from each of these components, applying the formula: $\tau_w = [(af.\tau_f) + (as.\tau_s)]/(af + as)$, where af and as are the relative amplitudes of the two exponential components and τf and τs are the corresponding time constants.

cAMP accumulation assay

Human embryonic kidney 293 cells stably expressing the D2R (*66*) were grown on polylysine (poly-D-lysine hydrobromide, Sigma-Aldrich) and transfected with Tet-On plasmids encoding either the D2R-IL3 or D2R-IL3-scr peptides and the Tag RFP (4 μg per well), complexed with Lipofectamine 2000 transfection reagent (Invitrogen), in Dulbecco's modified Eagle medium (DMEM, high glucose, GlutaMAX Supplement, pyruvate, Gibco), and incubated for 5 hours. After transfection, cells were rinsed and wells were filled with DMEM supplemented with 10% fetal bovine serum and antibiotics to induce D2R expression [hygromycin (2 μl/ml; Sigma-Aldrich), blasticidin (1.5 μl/ml; ant-bl-1, Cayla InvivoGen), and tetracycline (1 μl/ml; T7660-5g, Sigma-Aldrich)] and incubated overnight. Peptide expression was induced by addition of dox solution (1 μg/ml), incubating for 48 hours. Following the dox treatment, cells were rinsed in DMEM before pretreatment with 1 mM isobutylmethylxanthine (IBMX; Sigma-Aldrich) for 15 min. Cells were then stimulated for 30 min with the indicated concentrations of agonist quinpirole (Tocris), in the presence of 1 mM IBMX and 10 μM forskolin (Tocris). Endogenous phosphodiesterase activity was stopped by aspiration of the medium and the addition of 0.1 M HCl (300 μl per well). After centrifugation at 600*g* for 10 min, protein concentration of supernatants was quantified by BCA (Uptima, Interchim). cAMP levels were determined in samples containing 10 μg of protein. The accumulation of cAMP was measured using a cAMP Enzyme Immunoassay kit (Sigma-Aldrich) as described by the manufacturer using Victor3 (PerkinElmer) plate reader. The curve fit was obtained by GraphPad Prism 8 (GraphPad Software Inc.).

Statistical analysis

Results were analyzed with GraphPad Prism (version 8.0.1). Sample size was predetermined on the basis of published studies, pilot experiments, and in-house expertise. All data are displayed as means ± SEM. Two-tailed Student's *t* test was used for the comparison of two independent groups. For more than two group comparison, one-way, two-way, or three-way repeated-measures analysis of variance (ANOVA) was performed followed by Bonferroni post hoc test. Data distribution was assumed to be normal, and variances were assumed to be homogenous. The main effect and post hoc statistical

significances are given in the appropriate figure legend for each experiment.

SUPPLEMENTARY MATERIALS

Supplementary material for this article is available at https://science.org/doi/10.1126/sciadv.abg5970

View/request a protocol for this paper from *Bio-protocol*.

REFERENCES AND NOTES

1. C. Lüscher, R. C. Malenka, Drug-evoked synaptic plasticity in addiction: From molecular changes to circuit remodeling. *Neuron* **69**, 650–663 (2011).
2. M. Salery, P. Trifilieff, J. Caboche, P. Vanhoutte, From signaling molecules to circuits and behaviors: Cell-type-specific adaptations to psychostimulant exposure in the striatum. *Biol. Psychiatry* **87**, 944–953 (2020).
3. N. D. Volkow, M. Morales, The brain on drugs: From reward to addiction. *Cell* **162**, 712–725 (2015).
4. S. E. Hyman, R. C. Malenka, E. J. Nestler, Neural mechanisms of addiction: The role of reward-related learning and memory. *Annu. Rev. Neurosci.* **29**, 565–598 (2006).
5. J. Bertran-Gonzalez, C. Bosch, M. Maroteaux, M. Matamales, D. Herve, E. Valjent, J.-A. Girault, Opposing patterns of signaling activation in dopamine D1 and D2 receptor-expressing striatal neurons in response to cocaine and haloperidol. *J. Neurosci.* **28**, 5671–5685 (2008).
6. S. M. Ferguson, D. Eskenazi, M. Ishikawa, M. J. Wanat, P. E. M. Phillips, Y. Dong, B. L. Roth, J. F. Neumaier, Transient neuronal inhibition reveals opposing roles of indirect and direct pathways in sensitization. *Nat. Neurosci.* **14**, 22–24 (2011).
7. T. Hikida, K. Kimura, N. Wada, K. Funabiki, S. Nakanishi, Distinct roles of synaptic transmission in direct and indirect striatal pathways to reward and aversive behavior. *Neuron* **66**, 896–907 (2010).
8. A. V. Kravitz, L. D. Tye, A. C. Kreitzer, Distinct roles for direct and indirect pathway striatal neurons in reinforcement. *Nat. Neurosci.* **15**, 816–818 (2012).
9. M. K. Lobo, H. E. Covington, D. Chaudhury, A. K. Friedman, H. Sun, D. Damez-Werno, D. M. Dietz, S. Zaman, J. W. Koo, P. J. Kennedy, E. Mouzon, M. Mogri, R. L. Neve, K. Deisseroth, M.-H. Han, E. J. Nestler, Cell type-specific loss of BDNF signaling mimics optogenetic control of cocaine reward. *Science* **330**, 385–390 (2010).
10. R. Bock, J. H. Shin, A. R. Kaplan, A. Dobi, E. Markey, P. F. Kramer, C. M. Gremel, C. H. Christensen, M. F. Adrover, V. A. Alvarez, Strengthening the accumbal indirect pathway promotes resilience to compulsive cocaine use. *Nat. Neurosci.* **16**, 632–638 (2013).
11. P. F. Durieux, B. Bearzatto, S. Guiducci, T. Buch, A. Waisman, M. Zoli, S. N. Schiffmann, A. de Kerchove d'Exaerde, D2R striatopallidal neurons inhibit both locomotor and drug reward processes. *Nat. Neurosci.* **12**, 393–395 (2009).
12. P. F. Durieux, S. N. Schiffmann, A. de Kerchove d'Exaerde, Differential regulation of motor control and response to dopaminergic drugs by D1R and D2R neurons in distinct dorsal striatum subregions: Dorsal striatum D1R- and D2R-neuron motor functions. *EMBO J.* **31**, 640–653 (2012).
13. V. Pascoli, M. Turiault, C. Lüscher, Reversal of cocaine-evoked synaptic potentiation resets drug-induced adaptive behaviour. *Nature* **481**, 71–75 (2012).
14. V. Pascoli, J. Terrier, J. Espallergues, E. Valjent, E. C. O'Connor, C. Lüscher, Contrasting forms of cocaine-evoked plasticity control components of relapse. *Nature* **509**, 459–464 (2014).
15. V. Pascoli, A. Hiver, R. V. Zessen, M. Loureiro, R. Achargui, M. Harada, J. Flakowski, C. Lüscher, Stochastic synaptic plasticity underlying compulsion in a model of addiction. *Nature* **564**, 366–371 (2018).
16. J. Terrier, C. Lüscher, V. Pascoli, Cell-type specific insertion of GluA2-lacking AMPARs with cocaine exposure leading to sensitization, cue-induced seeking and incubation of craving. *Neuropsychopharmacology* **41**, 1779–1789 (2016).
17. C. L. Heusner, R. D. Palmiter, Expression of mutant NMDA receptors in dopamine D1 receptor-containing cells prevents cocaine sensitization and decreases cocaine preference. *J. Neurosci.* **25**, 6651–6657 (2005).
18. J. Schumann, R. Yaka, Prolonged withdrawal from repeated noncontingent cocaine exposure increases NMDA receptor expression and ERK activity in the nucleus accumbens. *J. Neurosci.* **29**, 6955–6963 (2009).
19. L. R. Beutler, M. J. Wanat, A. Quintana, E. Sanz, N. S. Bamford, L. S. Zweifel, R. D. Palmiter, Balanced NMDA receptor activity in dopamine D1 receptor (D1R)- and D2R-expressing medium spiny neurons is required for amphetamine sensitization. *Proc. Natl. Acad. Sci. U.S.A.* **108**, 4206–4211 (2011).
20. V. Pascoli, A. Besnard, D. Hervé, C. Pagès, N. Heck, J.-A. Girault, J. Caboche, P. Vanhoutte, Cyclic adenosine monophosphate–independent tyrosine phosphorylation of NR2B mediates cocaine-induced extracellular signal-regulated kinase activation. *Biol. Psychiatry* **69**, 218–227 (2011).
21. V. Pascoli, E. Cahill, F. Bellivier, J. Caboche, P. Vanhoutte, Extracellular signal-regulated protein kinases 1 and 2 activation by addictive drugs: A signal toward pathological adaptation. *Biol. Psychiatry* **76**, 917–926 (2014).
22. M. E. Joffe, S. R. Vitter, B. A. Grueter, GluN1 deletions in D1- and A2A-expressing cell types reveal distinct modes of behavioral regulation. *Neuropharmacology* **112**, 172–180 (2017).
23. A. Andrianarivelo, E. Saint-Jour, R. Walle, P. Trifilieff, P. Vanhoutte, Modulation and functions of dopamine receptor heteromers in drugs of abuse-induced adaptations. *Neuropharmacology* **152**, 42–50 (2019).
24. D. O. Borroto-Escuela, J. Carlsson, P. Ambrogini, M. Narváez, K. Wydra, A. O. Tarakanov, X. Li, C. Millón, L. Ferraro, R. Cuppini, S. Tanganelli, F. Liu, M. Filip, Z. Diaz-Cabiale, K. Fuxe, Understanding the role of GPCR heteroreceptor complexes in modulating the brain networks in health and disease. *Front. Cell. Neurosci.* **11**, 37 (2017).
25. S. Ferré, C. Quiroz, M. Orru, X. Guitart, G. Navarro, A. Cortés, V. Casadó, E. I. Canela, C. Lluis, R. Franco, Adenosine A(2A) receptors and A(2A) receptor heteromers as key players in striatal function. *Front. Neuroanat.* **5**, 36 (2011).
26. K. Fuxe, D. O. Borroto-Escuela, W. Romero-Fernandez, M. Palkovits, A. O. Tarakanov, F. Ciruela, L. F. Agnati, Moonlighting proteins and protein–protein interactions as neurotherapeutic targets in the g protein-coupled receptor field. *Neuropsychopharmacology* **39**, 131–155 (2014).
27. M. Wang, A. H. Wong, F. Liu, Interactions between NMDA and dopamine receptors: A potential therapeutic target. *Brain Res.* **1476**, 154–163 (2012).
28. F. J. S. Lee, S. Xue, L. Pei, B. Vukusic, N. Chéry, Y. Wang, Y. T. Wang, H. B. Niznik, X. Yu, F. Liu, Dual regulation of NMDA receptor functions by direct protein-protein interactions with the dopamine D1 receptor. *Cell* **111**, 219–230 (2002).
29. L. Pei, F. J. S. Lee, A. Moszczynska, B. Vukusic, F. Liu, Regulation of dopamine D1 receptor function by physical interaction with the NMDA receptors. *J. Neurosci.* **24**, 1149–1158 (2004).
30. C. Fiorentini, F. Gardoni, P. Spano, M. D. Luca, C. Missale, Regulation of dopamine D1 receptor trafficking and desensitization by oligomerization with glutamate N-methyl-D-aspartate receptors. *J. Biol. Chem.* **278**, 20196–20202 (2003).
31. E. Cahill, V. Pascoli, P. Trifilieff, D. Savoldi, V. Kappès, C. Lüscher, J. Caboche, P. Vanhoutte, D1R/GluN1 complexes in the striatum integrate dopamine and glutamate signalling to control synaptic plasticity and cocaine-induced responses. *Mol. Psychiatry* **19**, 1295–1304 (2014).
32. X.-Y. Liu, X.-P. Chu, L.-M. Mao, M. Wang, H.-X. Lan, M.-H. Li, G.-C. Zhang, N. K. Parelkar, E. E. Fibuch, M. Haines, K. A. Neve, F. Liu, Z.-G. Xiong, J. Q. Wang, Modulation of D2R-NR2B interactions in response to cocaine. *Neuron* **52**, 897–909 (2006).
33. P. Trifilieff, F. Ducrocq, S. van der Veldt, D. Martinez, Blunted dopamine transmission in addiction: Potential mechanisms and implications for behavior. *Semin. Nucl. Med.* **47**, 64–74 (2017).
34. P. Trifilieff, M.-L. Rives, E. Urizar, R. Piskorowski, H. Vishwasrao, J. Castrillon, C. Schmauss, M. Slättman, M. Gullberg, J. Javitch, Detection of antigen interactions ex vivo by proximity ligation assay: Endogenous dopamine D2-adenosine A2A receptor complexes in the striatum. *Biotechniques* **51**, 111–118 (2011).
35. A. S. Woods, F. Ciruela, K. Fuxe, L. F. Agnati, C. Lluis, R. Franco, S. Ferré, Role of electrostatic interaction in receptor-receptor heteromerization. *J. Mol. Neurosci.* **26**, 125–132 (2005).
36. T. E. Robinson, K. C. Berridge, The neural basis of drug craving: An incentive-sensitization theory of addiction. *Brain Res. Rev.* **18**, 247–291 (1993).
37. W.-D. Yao, R. R. Gainetdinov, M. I. Arbuckle, T. D. Sotnikova, M. Cyr, J.-M. Beaulieu, G. E. Torres, S. G. N. Grant, M. G. Caron, Identification of PSD-95 as a regulator of dopamine-mediated synaptic and behavioral plasticity. *Neuron* **41**, 625–638 (2004).
38. J. Zhang, T.-X. Xu, P. J. Hallett, M. Watanabe, S. G. N. Grant, O. Isacson, W.-D. Yao, PSD-95 uncouples dopamine-glutamate interaction in the D1/PSD-95/NMDA receptor complex. *J. Neurosci.* **29**, 2948–2960 (2009).
39. M. Dos Santos, M. Salery, B. Forget, M. A. Garcia Perez, S. Betuing, T. Boudier, P. Vanhoutte, J. Caboche, N. Heck, Rapid synaptogenesis in the nucleus accumbens is induced by a single cocaine administration and stabilized by mitogen-activated protein kinase interacting kinase-1 activity. *Biol. Psychiatry* **82**, 806–818 (2017).
40. S. Yagishita, A. Hayashi-Takagi, G. C. R. Ellis-Davies, H. Urakubo, S. Ishii, H. Kasai, A critical time window for dopamine actions on the structural plasticity of dendritic spines. *Science* **345**, 1616–1620 (2014).
41. E. J. Nestler, Molecular basis of long-term plasticity underlying addiction. *Nat. Rev. Neurosci.* **2**, 119–128 (2001).
42. M. B. Kelz, J. Chen, W. A. Carlezon, K. Whisler, L. Gilden, A. M. Beckmann, C. Steffen, Y.-J. Zhang, L. Marotti, D. W. Self, T. Tkatch, G. Baranauskas, D. J. Surmeier, R. L. Neve, R. S. Duman, M. R. Picciotto, E. J. Nestler, Expression of the transcription factor ΔFosB in the brain controls sensitivity to cocaine. *Nature* **401**, 272–276 (1999).
43. M. K. Lobo, S. Zaman, D. M. Damez-Werno, J. W. Koo, R. C. Bagot, J. A. DiNieri, A. Nugent, E. Finkel, D. Chaudhury, R. Chandra, E. Riberio, J. Rabkin, E. Mouzon, R. Cachope, J. F. Cheer, M.-H. Han, D. M. Dietz, D. W. Self, Y. L. Hurd, V. Vialou, E. J. Nestler, ΔFosB

induction in striatal medium spiny neuron subtypes in response to chronic pharmacological, emotional, and optogenetic stimuli. *J. Neurosci.* **33**, 18381–18395 (2013).
44. B. A. Grueter, A. J. Robison, R. L. Neve, E. J. Nestler, R. C. Malenka, ΔFosB differentially modulates nucleus accumbens direct and indirect pathway function. *Proc. Natl. Acad. Sci. U.S.A.* **110**, 1923–1928 (2013).
45. J. Kim, B.-H. Park, J. H. Lee, S. K. Park, J.-H. Kim, Cell type-specific alterations in the nucleus accumbens by repeated exposures to cocaine. *Biol. Psychiatry* **69**, 1026–1034 (2011).
46. Y. Zhu, J. Mészáros, R. Walle, R. Fan, Z. Sun, A. J. Dwork, P. Trifilieff, J. A. Javitch, Detecting G protein-coupled receptor complexes in postmortem human brain with proximity ligation assay and a Bayesian classifier. *Biotechniques* **68**, 122–129 (2019).
47. Y. Zhu, A. J. Dwork, P. Trifilieff, J. A. Javitch, Detection of G protein-coupled receptor complexes in postmortem human brain by proximity ligation assay. *Curr. Protoc. Neurosci.* **91**, e86 (2020).
48. G. F. Koob, N. D. Volkow, Neurobiology of addiction: A neurocircuitry analysis. *Lancet Psychiatry* **3**, 760–773 (2016).
49. N. D. Volkow, J. S. Fowler, A. P. Wolf, D. Schlyer, C. Y. Shiue, R. Alpert, S. L. Dewey, J. Logan, B. Bendriem, D. Christman, Effects of chronic cocaine abuse on postsynaptic dopamine receptors. *Am. J. Psychiatry* **147**, 719–724 (1990).
50. N. D. Volkow, G.-J. Wang, J. S. Fowler, J. Logan, S. J. Gatley, A. Gifford, R. Hitzemann, Y.-S. Ding, N. Pappas, Prediction of reinforcing responses to psychostimulants in humans by brain dopamine D2 receptor levels. *AJP* **156**, 1440–1443 (1999).
51. N. D. Volkow, G.-J. Wang, J. S. Fowler, D. Tomasi, F. Telang, Addiction: Beyond dopamine reward circuitry. *Proc. Natl. Acad. Sci. U.S.A.* **108**, 15037–15042 (2011).
52. M. Creed, N. R. Ntamati, R. Chandra, M. K. Lobo, C. Lüscher, Convergence of reinforcing and anhedonic cocaine effects in the ventral pallidum. *Neuron* **92**, 214–226 (2016).
53. A. F. MacAskill, J. M. Cassel, A. G. Carter, Cocaine exposure reorganizes cell type- and input-specific connectivity in the nucleus accumbens. *Nat. Neurosci.* **17**, 1198–1207 (2014).
54. M. K. Lobo, E. J. Nestler, The striatal balancing act in drug addiction: Distinct roles of direct and indirect pathway medium spiny neurons. *Front. Neuroanat.* **5**, 41 (2011).
55. P. Sun, J. Wang, W. Gu, W. Cheng, G. Jin, E. Friedman, J. Zheng, X. Zhen, PSD-95 regulates D 1 dopamine receptor resensitization, but not receptor-mediated Gs-protein activation. *Cell Res.* **19**, 612–624 (2009).
56. P. Paoletti, C. Bellone, Q. Zhou, NMDA receptor subunit diversity: Impact on receptor properties, synaptic plasticity and disease. *Nat. Rev. Neurosci.* **14**, 383–400 (2013).
57. A. L. Frederick, H. Yano, P. Trifilieff, H. D. Vishwasrao, D. Biezonski, J. Mészáros, E. Urizar, D. R. Sibley, C. Kellendonk, K. C. Sonntag, D. L. Graham, R. J. Colbran, G. D. Stanwood, J. A. Javitch, Evidence against dopamine D1/D2 receptor heteromers. *Mol. Psychiatry* **20**, 1373–1385 (2015).
58. P. W. Kalivas, K. McFarland, Brain circuitry and the reinstatement of cocaine-seeking behavior. *Psychopharmacology (Berl)* **168**, 44–56 (2003).
59. S. S. Song, B. J. Kang, L. Wen, H. J. Lee, H. Sim, T. H. Kim, S. Yoon, B.-J. Yoon, G. J. Augustine, J.-H. Baik, Optogenetics reveals a role for accumbal medium spiny neurons expressing dopamine D2 receptors in cocaine-induced behavioral sensitization. *Front. Behav. Neurosci.* **8**, 336 (2014).
60. F. Ciruela, J. Burgueño, V. Casadó, M. Canals, D. Marcellino, S. R. Goldberg, M. Bader, K. Fuxe, L. F. Agnati, C. Lluis, R. Franco, S. Ferré, A. S. Woods, Combining mass spectrometry and pull-down techniques for the study of receptor heteromerization. Direct epitope–epitope electrostatic interactions between adenosine A_{2A} and dopamine D_2 receptors. *Anal. Chem.* **76**, 5354–5363 (2004).
61. D. O. Borroto-Escuela, M. Narváez, K. Wydra, J. Pintsuk, L. Pinton, A. Jimenez-Beristain, M. Di Palma, J. Jastrzębska, M. Filip, K. Fuxe, Cocaine self-administration specifically increases A2AR-D2R and D2R-sigma1R heteroreceptor complexes in the rat nucleus accumbens shell. Relevance for cocaine use disorder. *Pharmacol. Biochem. Behav.* **155**, 24–31 (2017).
62. D. O. Borroto-Escuela, K. Wydra, X. Li, D. Rodriguez, J. Carlsson, J. Jastrzębska, M. Filip, K. Fuxe, Disruption of A2AR-D2R heteroreceptor complexes after A2AR transmembrane 5 peptide administration enhances cocaine self-administration in rats. *Mol. Neurobiol.* **55**, 7038–7048 (2018).
63. D. Belin, A. Belin-Rauscent, J. E. Murray, B. J. Everitt, Addiction: Failure of control over maladaptive incentive habits. *Curr. Opin. Neurobiol.* **23**, 564–572 (2013).
64. A. Dumais, A. D. Lesage, M. Alda, G. Rouleau, M. Dumont, N. Chawky, M. Roy, J. J. Mann, C. Benkelfat, G. Turecki, Risk factors for suicide completion in major depression: A case-control study of impulsive and aggressive behaviors in men. *AJP* **162**, 2116–2124 (2005).
65. J. K. Mai, G. Paxinos, T. Voss, *Atlas of the Human Brain* (Elsevier, Academic Press, ed. 3, 2008).
66. M. Michino, P. Donthamsetti, T. Beuming, A. Banala, L. Duan, T. Roux, Y. Han, E. Trinquet, A. H. Newman, J. A. Javitch, L. Shi, A single glycine in extracellular loop 1 Is the critical determinant for pharmacological specificity of dopamine D2 and D3 receptors. *Mol. Pharmacol.* **84**, 854–864 (2013).

Acknowledgments: We would like to thank the imaging facility of the IBPS and the histology facility of the Institut du Cerveau et de Moëlle épinière (ICM). **Funding:** This work was supported by the CNRS; the INSERM; Sorbonne Université, Faculté des Sciences et Ingénierie; Université de Bordeaux; Institut National de Recherche pour l'Agriculture, l'Alimentation et l'Environnement (INRAE); Université Côte d'Azur; the Agence Nationale pour la Recherche (ANR; ANR-15-CE16-001 to P.V. and P.T., ANR-18-CE37-0003-02 to J.B. and P.V., and ANR-10-IDEX-03-02 and ANR-16-CE16–0022 to P.T.); the Fondation pour la Recherche Médicale (FRM; DPA20140629798 to J.C. and DEQ20180339159 to J.B.); Institut de Recherche en Santé publique (IReSP) Aviesan APP-addiction 2019 (to P.V., P.T., and J.B.); NARSAD Young Investigator Grants from the Brain and Behavior Foundation (to P.T.); the BioPsy LabEx excellence cluster (to J.C. and P.V.); the LabEx BRAIN (to P.T.); NIH grant MH54137 (to J.A.J.); and the Hope for Depression Research Foundation (to J.A.J.). The DBCBB is funded by platform support grants from the RQSHA and HBHL (CFREF). A.A. and R.W. are recipients of PhD fellowships from the French Ministry of Research. A.P. is a recipient of a PhD fellowship from the "Ecole Universitaire de Recherche" (EUR Neuro, Bordeaux Neurocampus). E.S.-J. is the recipient of a fourth-year PhD fellowship from the FRM. **Authors contributions:** A.A. performed most PLA, viral injections, behavioral studies, immunohistochemistry, confocal imaging, and biochemistry and statistical analysis with the help of E.S.-J., M.-C.A., V.K, S.B., V.O., and R.W. Dendritic spine analysis was performed by N.H. and A.A. Electrophysiological recordings were performed by P.P. and S.P.F. Viruses were designed by P.V. and A.-P.B. and produced by C.J. and A.-P.B., and cAMP assays were performed by V.D.S.-P. and A.P. G.T and N.M. obtained, characterized, and provided human brain samples. Y.Z. and J.A.J. helped A.A. for PLA experiments from human tissues and related quantifications. A.A., J.C., P.T., J.B., and P.V. designed experiments and wrote the manuscript, which was edited by the other authors. **Competing interests:** The authors declare that they have no competing interests. **Data and materials availability:** All data needed to evaluate the conclusions in the paper are present in the paper and/or the Supplementary Materials.

Submitted 15 January 2021
Accepted 30 August 2021
Published 20 October 2021
10.1126/sciadv.abg5970

Citation: A. Andrianarivelo, E. Saint-Jour, P. Pousinha, S. P. Fernandez, A. Petitbon, V. De Smedt-Peyrusse, N. Heck, V. Ortiz, M.-C. Allichon, V. Kappès, S. Betuing, R. Walle, Y. Zhu, C. Joséphine, A.-P. Bemelmans, G. Turecki, N. Mechawar, J. A. Javitch, J. Caboche, P. Trifilieff, J. Barik, P. Vanhoutte, Disrupting D1-NMDA or D2-NMDA receptor heteromerization prevents cocaine's rewarding effects but preserves natural reward processing. *Sci. Adv.* **7**, eabg5970 (2021).

ScienceAdvances

Disrupting D1-NMDA or D2-NMDA receptor heteromerization prevents cocaine's rewarding effects but preserves natural reward processing

Andry AndrianariveloEstefani Saint-JourPaula PousinhaSebastian P. FernandezAnna PetitbonVeronique De Smedt-PeyrusseNicolas HeckVanesa OrtizMarie-Charlotte AllichonVincent KappèsSandrine BetuingRoman WalleYing ZhuCharlène JoséphineAlexis-Pierre BemelmansGustavo TureckiNaguib MechawarJonathan A. JavitchJocelyne CabochePierre TrifilieffJacques BarikPeter Vanhoutte

Sci. Adv., 7 (43), eabg5970.